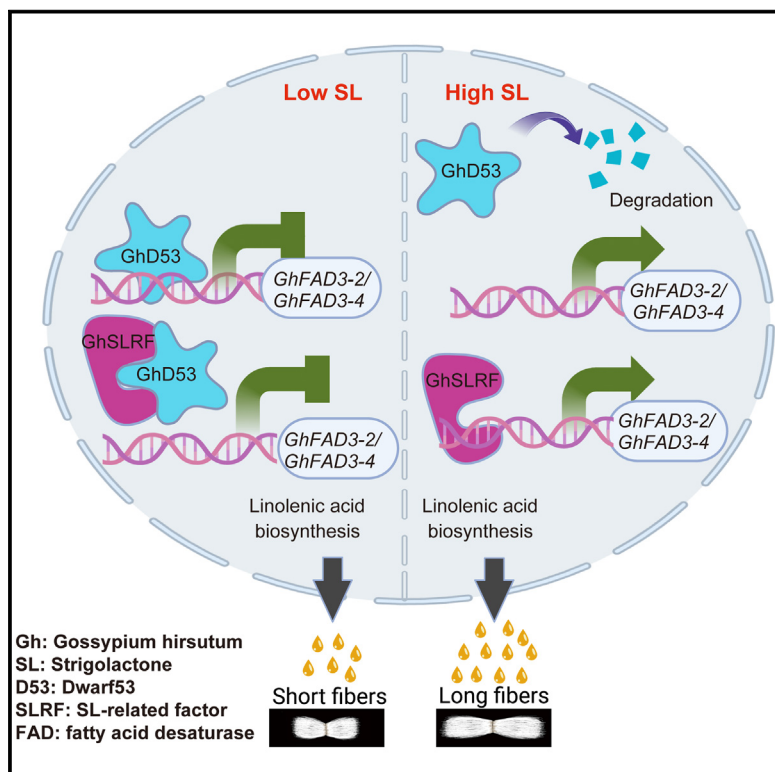


Strigolactone promotes cotton fiber cell elongation by de-repressing DWARF53 on linolenic acid biosynthesis

Graphical abstract



Authors

Huiqin Wang, Liping Zhu,
Mengyuan Fan, ..., Rezwan Tanvir,
Ling Li, Guanghui Xiao

Correspondence

guanghuix@snnu.edu.cn

In brief

Wang et al. identify that GhD53 functions as a transcriptional repressor and interacts with transcriptional activator GhSLRF to repress *GhFAD3* gene transcription. Strigolactone releases the transcription repression of GhD53 on *GhFAD3* and promotes cotton fiber elongation.

Highlights

- GhD53 functions as a suppressor, inhibiting SL-promoted fiber cell elongation
- GhD53 blocks the transcription of *GhFAD3* and inhibits C18:3 biosynthesis
- GhSLRF interacts with GhD53 and promotes transcription of *GhFAD3*
- Strigolactone releases the transcription repression of GhD53 on *GhFAD3*

Article

Strigolactone promotes cotton fiber cell elongation by de-repressing DWARF53 on linolenic acid biosynthesis

Huiqin Wang,^{1,3} Liping Zhu,^{1,3} Mengyuan Fan,^{1,3} Shuangshuang Weng,¹ Xin Zhou,¹ Hanxuan Zhao,¹ Yongcui Shen,¹ Jiaquan Chai,¹ Liyong Hou,¹ Miaoqiao Hao,¹ Rezwan Tanvir,² Ling Li,² and Guanghui Xiao^{1,4,*}

¹College of Life Sciences, Shaanxi Normal University, Xi'an 710062, China

²Department of Biological Sciences, Mississippi State University, Mississippi State, MS 39762, USA

³These authors contributed equally

⁴Lead contact

*Correspondence: guanghuix@snnu.edu.cn

<https://doi.org/10.1016/j.devcel.2024.12.009>

SUMMARY

Strigolactone (SL) is a plant hormone required for plant development. DWARF53 (D53) functions as a transcription repressor in SL signaling. However, the role of D53 in cotton (*Gossypium hirsutum*, Gh) fiber development remains unclear. Here, we identify that GhD53 suppresses fiber elongation by repressing transcription of *GhFAD3* genes, which control linolenic acid (C18:3) biosynthesis. Mechanistically, GhD53 interacts with SL-related transcriptional activate factor (GhSLRF) to prevent its binding on Omega-3 fatty acid desaturase gene (*GhFAD3*) promoters, thereby inhibiting *GhFAD3* transcription. Upon SL exposure, GhD53 is degraded and leads to GhSLRF activation. This activation further promotes *GhFAD3* transcription, C18:3 biosynthesis, and fiber elongation. Our findings identify the molecular mechanism of how SL controls cell elongation via D53 and offer potential strategies to improve cotton quality through SL application.

INTRODUCTION

Cell elongation, a fundamental cellular process for driving plant growth, is crucial for organ development and growth.¹ Dynamic nature of plant cell elongation encompasses changes in both rate and direction throughout development and in response to external environmental cues.² Given its unique attributes, cotton fiber serves as an excellent model for investigating plant single-cell elongation.³ Furthermore, upland cotton (*Gossypium hirsutum*, Gh) fibers hold significant commercial value as the primary natural raw material utilized in the textile industry.⁴ With our expanding knowledge of cotton genomes, it is becoming increasingly feasible to genetically enhance the fiber characteristics of Gh, such as its length, fineness, and strength, rather than relying solely on traditional breeding methods.

Cotton fiber development consists of four interconnected stages: initiation, elongation, secondary cell wall synthesis, and maturation.⁵ Notably, fiber cell differentiation commences within the outer integument approximately 2–3 days prior to anthesis, with active growth commencing within 0–3 days post-anthesis (DPA). Following initiation, these fiber cells enter a phase of rapid elongation, persisting until around 20 DPA, a pivotal stage in fiber cell development. At approximately 15 DPA, these cells begin to synthesize substantial quantities of cellulose, leading to thickening of fiber cell walls and marking the onset of the secondary cell wall synthesis stage. During the maturation stage (45–60 DPA), fibers undergo dehydration and maturation processes.⁶

Phytohormones play a critical role in plant growth, development, and responses to external stimuli.⁷ Among them, strigolactone (SL) holds a prominent position in regulating plant growth and development. SL exerts profound effects on fungal symbiosis, shoot branching, anthocyanin accumulation, root architecture, leaf development, flower size, plant height, and adaptation to drought, heat tolerance, freezing tolerance, and phosphate scarcity.^{8–15} Biosynthesis of SL starts from carotenoid pathway: the enzyme carotenoid isomerase Dwarf27 converts all-trans-β-carotene into 9-cis-β-carotene.¹⁰ Subsequently, this precursor is transformed into carlactone by carotenoid cleavage dioxygenase 8.¹⁶ Successive enzymatic conversions lead to production of 5-deoxylstrigol and other bioactive SL, facilitated by a cytochrome P450 monooxygenase encoded by *More Axillary Growth 1*.¹⁷

Perception of SL relies on α/β-hydrolase DWARF14, serving as the switch that initiates the SL signaling cascade. This leads to the formation of a complex involving D3, an F-box protein integral to the Skp-Cullin-F-box (SCF) E3 ubiquitin ligase, and the repressor DWARF53 (D53).¹⁸ D53 physically interacts with transcription factor proteins.¹⁹ SCFD3-D14-D53 complex triggers polyubiquitination and subsequent degradation of D53. This degradation, in turn, activates transcriptional activity of specific transcription factors, thereby triggering transcriptional activation of SL-responsive genes previously repressed by D53, thereby facilitating growth responses to SL.²⁰

D53 proteins exhibit limited similarity to class 1 Hsp100/ClpB proteins and play a crucial role in repressing SL signaling

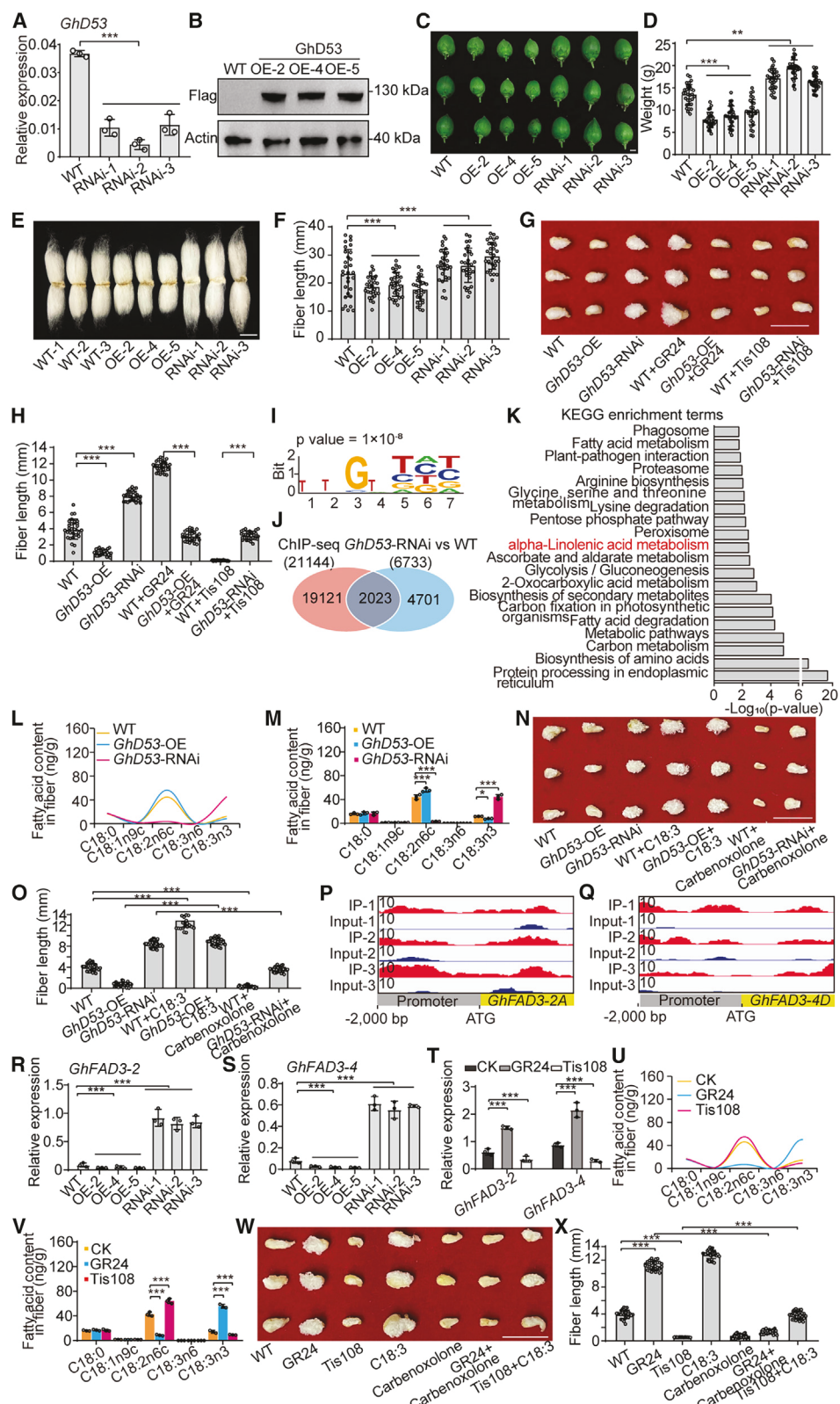


Figure 1. *GhD53* as a negative regulator of cotton fiber cell elongation

(A) Relative expression level of *GhD53* in wild-type (WT) and *GhD53*-RNAi transgenic cotton plants. DPA, day-post-anthesis.

(B) Western blot analysis of *GhD53* protein in 10-DPA fibers from WT and *GhD53*-OE transgenic cotton plants.

(legend continued on next page)

pathway, thereby regulating downstream transcriptional network of SL responses.^{21,22} Suppressor of MAX2 1-like (SMXL) proteins contain conserved ethylene-response elements binding factor-associated amphiphilic repression (EAR) motifs, widely recognized as essential contributors to SMXL function.^{9,11,22,23} Interactions between SMXL1 and SMXL7 with TOPLESS-RELATED PROTEIN2 (TPR2), as well as those involving SMXL6, SMXL7, and SMXL8 with TPR2, all hinge on EAR-motif-dependent interaction.^{23,24} In *Arabidopsis*, the repression exerted by SMXL6 on the SMXL7 promoter is also contingent on the presence of EAR motif.⁹

SL has emerged as crucial regulators to stimulate plant cell elongation. In *Arabidopsis*, SL interacts with ethylene and auxin to finely regulate root-hair elongation.²⁵ Gibberellin, on the other hand, boosts SL biosynthesis to promote fiber cell elongation.^{26,27} For internode elongation in *Pisum sativum*, the SL has been reported to stimulate this process independently of gibberellin pathway.²⁸ However, the precise role and regulatory mechanism of SMXL/D53 in SL-regulated single-cell elongation have remained elusive.

In this study, we present evidence that GhD53 functions as a suppressor, inhibiting SL-promoted fiber cell elongation. Together, our study identified a regulatory mechanism of D53-mediated SL signaling cascade in controlling plant development at single-cell level. It offers a promising strategy to improve the yield and quality of cotton fibers, which could directly benefit the textile industry.

RESULTS

GhD53 inhibits cotton fiber cell elongation by repressing linolenic acid biosynthesis

In Gh, six distinct *D53* genes exist. Phylogenetic analysis of these *D53* genes in cotton and *Arabidopsis* showed that GhD53-5 and GhD53-6 shared the closest phylogenetic relationship, while GhD53-1 to GhD53-4 exhibited a closer phylogenetic

connection (Figure S1A). Interestingly, four of these *GhD53* genes (GhD53-3, GhD53-4, GhD53-5, and GhD53-6) displayed notably high expression levels during ovule and fiber development stages (Figure S1B). Further examination via multiple sequence alignments identified the presence of four conserved domains within D53 proteins (Figure S1C). Our study demonstrated that among these GhD53 variants, only GhD53-6 possessed the capacity to bind to its own promoter (Figure S1D) and enacted negative regulation of its own transcription (Figure S1E). Moreover, the GhD53-6 protein accumulation was reduced after synthetic strigolactone analog rac-GR24 (GR24) treatment (Figure S1F). The suitable concentration of GR24 is 15 μ M, which has been reported in previous research.²⁶ Consequently, for the purposes of this investigation, we have selected GhD53-6, GhD53 hereafter.

Subcellular localization assays confirmed that GhD53 protein predominantly localized within nucleus of tobacco leaves (Figure S1G). The GhD53 exhibited predominant expression within cotton fibers at the critical developmental stage of 10–20 DPA (Figure S1H), while the accumulation of GhD53 protein decreased gradually as cotton fiber growth progressed (Figure S1I). GR24 treatment enhanced transcripts of *GhD53*, and Tis108 reduced *GhD53* expression (Figure S1J).

To gain deeper insights into the impact of GhD53 on cotton fiber development, we successfully generated the *GhD53*-OE plants and *GhD53* RNA interference lines (*GhD53*-RNAi) (Figures 1A, 1B, and S1K–S1N). The lint percentage in *GhD53* transgenic lines was comparable to that of wild-type plants (Figure S1O). Overexpression of *GhD53* resulted in a decrease in cotton ball weight (Figures 1C and 1D), mature fiber length (Figures 1E and 1F), fiber initiation, plant height, and seed weight (Figures S1P–S1V). By contrast, reducing *GhD53* transcripts resulted in the opposite phenotype.

Additionally, we observed that overexpressing *GhD53* attenuated the positive effects of GR24 on fiber growth, while the interference with *GhD53* gene expression partially mitigated the

(C) Images of 10-DPA cotton bolls from WT, *GhD53*-OE, and *GhD53*-RNAi cotton plants.

(D) Statistical analysis of the weight of cotton bolls in (C).

(E) Image of mature fiber cells from WT, *GhD53*-OE, and *GhD53*-RNAi cotton plants.

(F) Statistical analysis of fiber length in (E).

(G) Image of fibers from WT and *GhD53* transgenic plants treated with GR24 or Tis108 for 10 days.

(H) Statistical analysis of fiber length in (G).

(I) Identification of potential *GhD53*-binding motif with 1 kb flanking sequences around each bound peak. The number of binding region peaks (peak count frequency) corresponds to the indicated region.

(J) Venn diagram showing the extent of overlap between genes identified from ChIP-seq and RNA-seq.

(K) Kyoto Encyclopedia of Genes and Genomes (KEGG) enrichment analysis of 202 genes upregulated in fiber elongation stage.

(L) Fatty acid (C18) content in 10-DPA fibers from *GhD53* transgenic and WT cotton plants.

(M) Statistical analysis of fatty acid content in (L).

(N) Fiber images from WT and *GhD53* transgenic plants after treatment with C18:3 or C18:3 inhibitor for 10 days.

(O) Statistical analysis of fiber length in (N).

(P and Q) Integrative Genomics Viewer (IGV) images showing binding peaks of *GhD53* in the *GhFAD3-2* (P) and *GhFAD3-4* (Q) promoter. IGV 2.12.0 is used for visualizing the binding peaks.

(R–T) Relative expression level of *GhFAD3-2* (R) and *GhFAD3-4* (S) in 10-DPA fibers from WT and *GhD53* transgenic cotton plants and from WT plants after treatment with GR24 or Tis108 for 10 days (T).

(U) Fatty acid (C18) content in fibers treated with GR24 or Tis108 for 10 days. CK, control.

(V) Statistical analysis of fatty acid content in (U).

(W) Fiber images from WT plants after treatment with C18:3 or carbenoxolone (C18:3 biosynthesis inhibitor) in combination with GR24 or Tis108 for 10 days.

(X) Statistical analysis of fiber length in (W).

In (A), (D), (F), (H), (M), (O), (R)–(T), (V), and (X), values are means \pm SD ($n = 3$ for A, M, R–T, and V and $n = 30$ for D, F, H, O, and X). *** and ** indicate $p < 0.001$ and $p < 0.01$ (Student's t test). In (C), (E), (G), (N), and (W), scale bar, 10 mm.

See also Figures S1–S3 and Tables S1, S2, and S3.

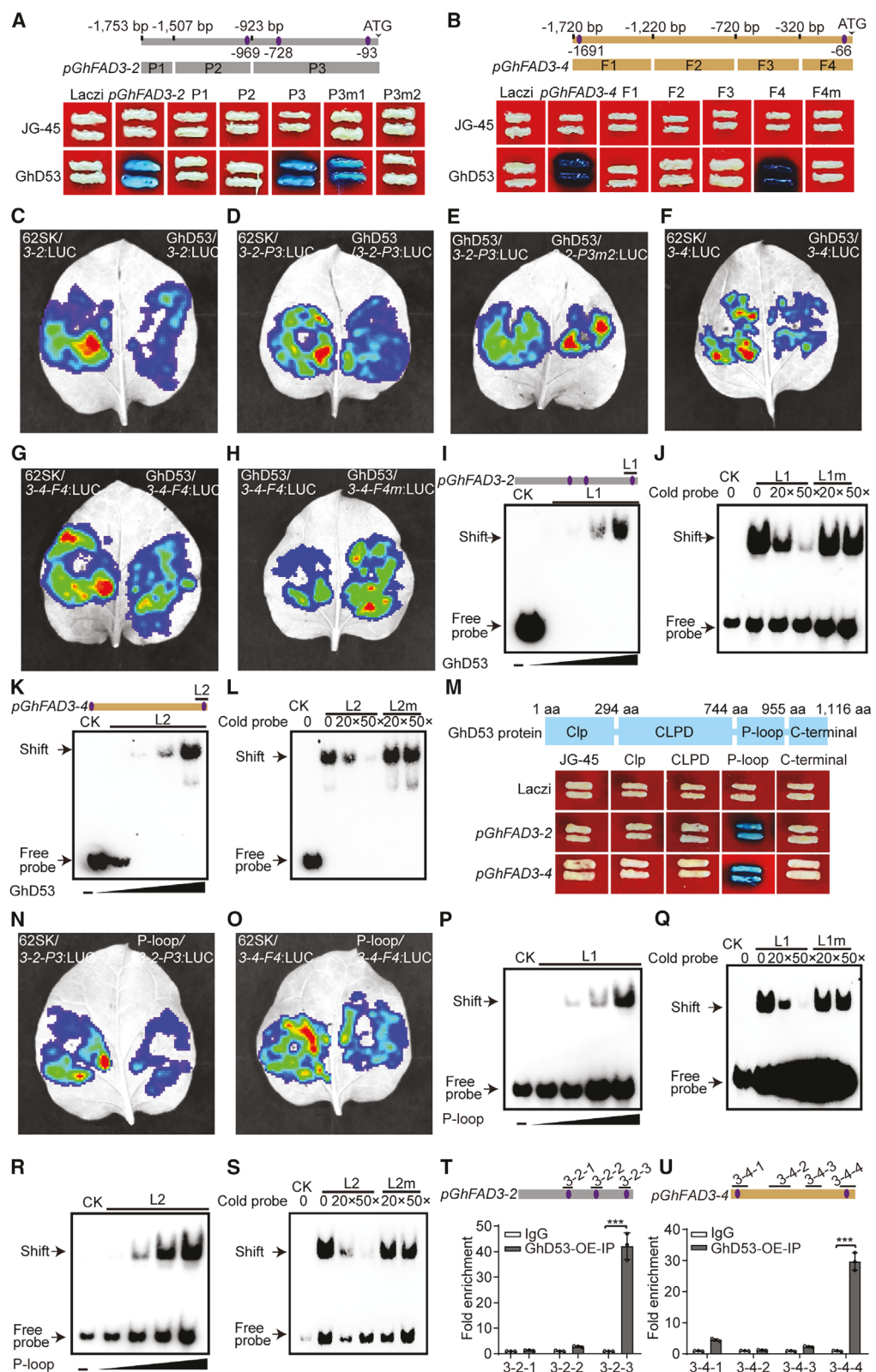


Figure 2. GhD53 protein directly binds to GhFAD3-2 and GhFAD3-4 promoters

(A and B) Yeast one-hybrid assay showing the binding of GhD53 to full length and fragments of *GhFAD3-2* (A) or *GhFAD3-4* (B) promoter. The purple ovals represent the GhD53-binding sites.

(legend continued on next page)

Developmental Cell

Article



inhibitory effects of Tis108 (an SL biosynthesis inhibitor) on fiber elongation (Figures 1G and 1H).²⁹ These findings suggest that GhD53 functions as a negative regulator, mediating the SL signal, and thereby plays a pivotal role in regulating fiber development.

Given GhD53's capability to regulate its target gene expression by binding to promoters, we conducted chromatin immunoprecipitation sequencing (ChIP-seq) and RNA sequencing (RNA-seq) analyses on *GhD53* transgenic cotton plants (Figures 1I and 1J; Figures S2A–S2C). Subsequently, we investigated expression patterns of these overlapping genes across various fiber development stages and identified 202 genes with high expression levels (Fragments Per Kilobase of exon model per Million mapped fragments, FPKM > 15) during fiber elongation stage (10-DPA fiber) (Figure S2D; Table S1). An enrichment analysis of Kyoto Encyclopedia of Genes and Genomes (KEGG) terms underscored that GhD53 target genes are predominantly associated with alpha-linolenic acid metabolism pathway (Figure 1K). Additionally, we identified two linolenic acid biosynthesis genes (*GhFAD3-2A* and *GhFAD3-4D*) within the enriched pathways, each containing the TTGTTAT (ATAACAA) element in their promoter regions (Figures S2E and S2F). We conducted DNA affinity purification sequencing (DAP-seq) analyses in parallel (Figures S2G–S2I).

Additionally, we conducted RNA-seq analysis of fibers treated with GR24 or Tis108 and identified 24,485 differentially expressed genes (DEGs). Among them, 481 were upregulated and 751 were downregulated following GR24 treatment, while 6,088 were upregulated and 17,165 were downregulated after Tis108 treatment. Subsequent KEGG pathway enrichment analysis highlighted that these enriched DEGs were involved in fatty acid elongation pathways (Figures S2J–S2N; Tables S2 and S3).

These results strongly indicate that GhD53 serves as a mediator of SL signal to regulate linolenic acid biosynthesis. This conclusion is substantiated by a comparison of fatty acid content profiles, which displayed significantly lower levels of linolenic acid (C18:3) in *GhD53-OE* transgenic cotton fibers compared with wild type (Figures 1L and 1M). Remarkably, application of C18:3 successfully restored shortened cotton fibers resulting from *GhD53* overexpression (Figures 1N and

1O). Furthermore, treatment with C18:3 significantly enhanced fiber elongation in *GhD53*-RNAi cotton fibers (Figures S2O and S2P). *GhD53*-RNAi transgenic cotton and application inhibitors Tis108 and carbenoxolone, the opposite conclusion is true.

Within genes associated with fatty acid synthesis, *FAD3* plays a crucial role in catalyzing synthesis of C18:3 from C18:2 (Figure S2Q).³⁰ In cotton, there are 11 *FAD3* genes, with *GhFAD3-2A/D* (*GhFAD3-2*) and *GhFAD3-4A/D* (*GhFAD3-4*) showing a striking 57.37% protein sequence similarity and high expression levels during fiber elongation (Figures S2R and S2S). Importantly, ChIP-seq peak analyses found that GhD53 had a strong affinity for promoters of *GhFAD3-2* and *GhFAD3-4* (Figures 1P and 1Q).

Collectively, cotton fibers subjected to GR24 treatment or derived from *GhD53*-RNAi transgenic plants displayed increased *GhFAD3-2* and *GhFAD3-4* transcripts, whereas Tis108 treatment or overexpression of *GhD53* led to a reduction in their transcriptional expression (Figures 1R–1T). In parallel, the accumulation of C18:3 was enhanced by GR24 treatment but decreased following Tis108 treatment (Figures 1U and 1V). Notably, the C18:3 inhibitor carbenoxolone suppressed the GR24-induced fiber elongation, while the addition of C18:3 mitigated the inhibitory effect of Tis108 on fiber elongation (Figures 1W and 1X). Moreover, C18:3 significantly enhanced the GR24-induced fiber elongation, while treatment with carbenoxolone and Tis108 completely inhibited fiber cell elongation (Figures S3A and S3B). Altogether, these findings strongly support the notion that C18:3 operates downstream of GhD53-mediated SL pathway, exerting regulatory control over fiber cell elongation.

***GhFAD3-2* and *GhFAD3-4* are two major targets of GhD53 that regulate SL-mediated fiber cell elongation**

Prior research has documented D53 protein's binding affinity for ATAACAA element within target gene promoters.⁹ In our study, we identified three and two TTGTTAT (ATAACAA) elements within *GhFAD3-2* and *GhFAD3-4* promoters, respectively (Figures S2E and S2F). To validate binding activity between GhD53 and *GhFAD3-2* and *GhFAD3-4* promoters, we conducted Yeast one-hybrid (Y1H) assay. The results demonstrated that GhD53 not only directly bound to full length, P3, and

(C–H) Tobacco transient expression assay of GhD53 and *GhFAD3-2* promoter (C), of GhD53 and *GhFAD3-2* promoter fragments with native (D) or mutated (E) binding site, of GhD53 and *GhFAD3-4* promoter (F), and of GhD53 and *GhFAD3-4* promoter fragments with intact (G) or mutated (H) binding site.

(I and K) Electrophoretic mobility shift assay (EMSA) demonstrating GhD53's direct binding to the L1 fragment of the *GhFAD3-2* promoter (I) and the L2 fragment of the *GhFAD3-4* promoter (K). CK, control.

(J and L) Competitive EMSA assay using a biotin-labeled L1 fragment of the *GhFAD3-2* promoter (J) and a biotin-labeled L2 fragment of the *GhFAD3-4* promoter (L) incubated with GhD53, competing with different concentrations of cold probes (without biotin label) containing the intact or mutated binding site (L1m, J or L2m, L).

(M) Yeast one-hybrid assay demonstrating the binding of four domains of GhD53 to the *GhFAD3-2* and *GhFAD3-4* promoters.

(N and O) Tobacco transient expression assay identifying the interaction of GhD53's P-loop domain with the *GhFAD3-2-P3* promoter fragment (N) and the *GhFAD3-4-F4* promoter fragment (O).

(P and R) EMSA assay showing that GhD53's P-loop domain directly binds to the L1 fragment of *GhFAD3-2* promoter (P) and the L2 fragment of *GhFAD3-4* promoter (R).

(Q and S) Competitive EMSA assay using a biotin-labeled L1 fragment of the *GhFAD3-2* promoter (Q) and a biotin-labeled L2 fragment of the *GhFAD3-4* promoter (S) incubated with the P-loop domain, competing with different concentrations of cold probes (without biotin label) of intact or mutated binding site (L1m, Q and L2m, S).

(T and U) ChIP-qPCR analysis showing a high degree of enrichment in the 3-2-3 region of *GhFAD3-2* promoter (T) and 3-4-4 region of *GhFAD3-4* promoter (U) in *GhD53-OE* lines. Values are means \pm SD ($n = 3$). Student's t test was used to calculate the p values, *** $p < 0.001$. 3-2, *GhFAD3-2* promoter region; 3-4, *GhFAD3-4* promoter region.

See also Figure S3.

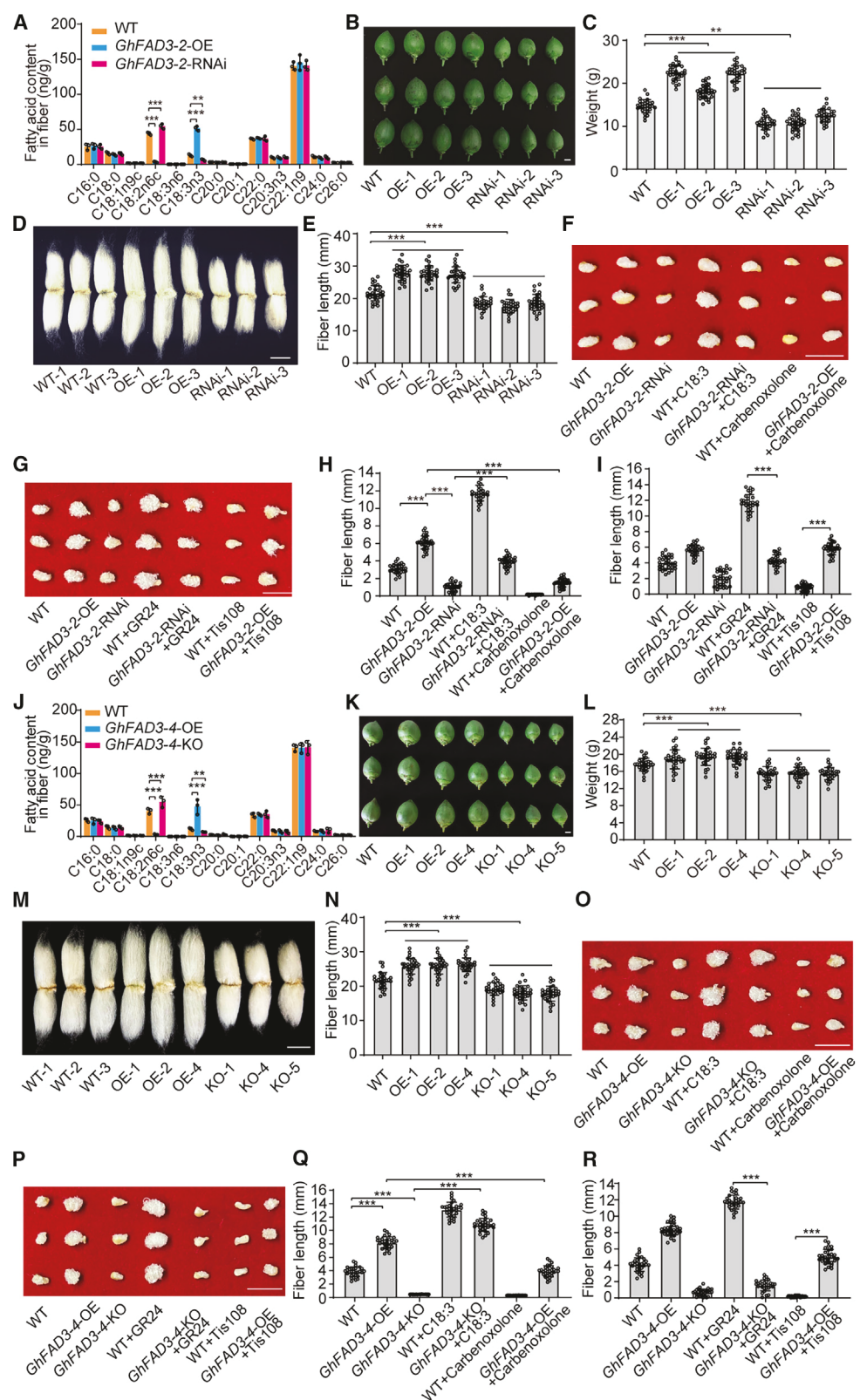


Figure 3. GhFAD3-2 promotes fiber cell elongation in cotton

(A) Fatty acid content in 10-DPA fibers of WT and GhFAD3-2 transgenic cotton plants.
(B) Images of 10-DPA cotton bolls of WT and GhFAD3-2 transgenic cotton plants.

(legend continued on next page)

Developmental Cell

Article



P3m1 (which contained a mutation in the first binding site) fragments of *GhFAD3-2* promoter but also interacted with full length and F4 fragment of *GhFAD3-4* promoter (Figures 2A and 2B). Notably, these binding interactions were disrupted when second binding site of P3 was mutated (P3m2) or when binding site within F4 was mutated (F4m). These direct binding interactions were further validated by tobacco transient and dual-luciferase assays (Figures 2C–2H and Figures S3C–S3H). Electrophoretic mobility shift assay (EMSA) provided additional evidence of the binding affinity between GhD53 protein and L1 and L2 probes. Critically, mutations within their TTGTTAT (ATAACAA) binding site abolished their interaction with GhD53 (Figures 2I–2L).

GhD53 protein encompasses four conserved domains. Y1H assays, combined with tobacco transient and dual-luciferase assays, identified that P-loop domain possessed capability to bind to both *GhFAD3-2* and *GhFAD3-4* promoters (Figures 2M–2O and S3I and S3J). EMSA further affirmed these above interactions (Figures 2P–2S). The ChIP-quantitative real-time polymerase chain reaction (ChIP-qPCR) demonstrated that *GhFAD3-2* promoter fragment, containing the third binding site, and *GhFAD3-4* promoter fragment, containing the second binding site of GhD53, could be significantly enriched in *GhD53*-OE fibers (Figures 2T and 2U). Considering the recognized importance of EAR motif in D53's binding to target genes,^{9,19,22} we conducted investigations to assess the impact of EAR motif on GhD53's binding to *GhFAD3-2* and *GhFAD3-4* promoters. Notably, P-loop with a mutated EAR-2 motif lost its ability to bind to *GhFAD3-2*-P3 and *GhFAD3-4*-F4 fragments, implying the critical role of EAR-2 motif in GhD53's interaction with *GhFAD3-2* and *GhFAD3-4* promoters (Figure S3K).

Collectively, these findings pointed to the pivotal role of P-loop domain within GhD53 protein for its binding to the third TTGTTAT (ATAACAA) *cis*-element within *GhFAD3-2* promoter and the second *cis*-element within *GhFAD3-4* promoter.

Furthermore, subcellular localization of *GhFAD3-2* and *GhFAD3-4* at the cytomembrane was confirmed (Figure S4A). Both *GhFAD3-2* and *GhFAD3-4* can promote the biosynthesis of C18:3 (Figures S4B–S4E). The C18:3 content primarily accumulated in fibers during the elongation stage (Figure S4F). The RT-qPCR analysis found that *GhFAD3-2* exhibited high expression levels in 15-DPA fibers (Figure S4G), indicating its involvement in cotton fiber elongation. To investigate *GhFAD3-2*'s function in cotton, *GhFAD3-2* overexpressing (*GhFAD3-2*-OE) and RNAi (*GhFAD3-2*-RNAi) transgenic cotton plants were gener-

ated (Figures S4H–S4K). Utilizing CRISPR-Cas9 system for a complete knockout of *GhFAD3-2* gene resulted in the generation of callus from cotton hypocotyl, yet these callus formations displayed an inability to differentiate into buds. After many such attempts failed, we prepared *GhFAD3-2* gene silencing material (*GhFAD3-2*-RNAi). Results showed that overexpression of *GhFAD3-2* enhanced accumulation of *GhFAD3-2* transcripts and protein, as well as linolenic acid C18:3 content, resulting in increased cotton boll weight, fiber cell length and initiation, plant height, and mature seed weight; conversely, suppression of *GhFAD3-2* transcription led to contrary conclusions (Figures 3A–3E and S4L–S4S). C18:3 rescued short fiber length observed in *GhFAD3-2*-RNAi lines and promoted fiber elongation in *GhFAD3-2*-OE cottons, while C18:3 inhibitor (carbenoxolone) reduced long fiber phenotype in *GhFAD3-2*-OE lines and suppressed fiber elongation in *GhFAD3-2*-RNAi cottons (Figures 3F, 3H, S4T, and S4U). Compared with GR24-treated wild type, *GhFAD3-2*-RNAi cotton treated with GR24 produced much shorter fibers. By contrast, following Tis108 treatment, *GhFAD3-2*-OE cotton produced longer fibers relative to wild type (Figures 3G and 3I).

Moreover, *GhFAD3-4* exhibited predominant expression in cotton fiber during its elongation stage (5–15 DPA) (Figure S4V). Subsequently, transgenic plants overexpressing or knocking out *GhFAD3-4* were generated (Figures S4W–S4AA). Analogous to outcomes observed in *GhFAD3-2* overexpressing lines, overexpression of *GhFAD3-4* led to increase of linolenic acid content, cotton boll weight, fiber length, plant height, seed weight, and fiber initiation (Figures 3J–3N and S4AB–S4AI). Conversely, knockout of *GhFAD3-4* resulted in a significant decrease of linolenic acid content, cotton boll weight, fiber length, plant height, seed weight, and fiber initiation (Figures 3J–3N and S4AB–S4AI).

In *vitro* ovule culture, C18:3 supplementation could rescue the short fiber length in *GhFAD3-4*-KO lines, while C18:3 inhibitor reduced extended fiber phenotype in *GhFAD3-4*-OE lines (Figures 3O and 3Q). Furthermore, following GR24 treatment, *GhFAD3-4*-KO plants produced shorter fibers compared with wild type, while in contrast to wild type, *GhFAD3-4*-OE lines exhibited significant resistance to negative effects of Tis108 on fiber elongation (Figures 3P and 3R). These cumulative results provide strong evidence that *GhFAD3-2* and *GhFAD3-4* serve as positive regulators downstream of SL signal in cotton fiber development.

(C) Statistical analysis of cotton boll weight in (B).

(D) Image of mature fiber cells from WT and *GhFAD3-2* transgenic cotton plants.

(E) Statistical analysis of fiber length in (D).

(F and G) Image of fibers of WT and *GhFAD3-2* transgenic plants treated with C18:3 or C18:3 biosynthesis inhibitor (F) and with GR24 or Tis108 (G) for 10 days.

(H and I) Statistical analysis of fiber length in (F) and (G), respectively.

(J) Fatty acid content in 10-DPA fibers from WT and *GhFAD3-4* transgenic cotton plants.

(K) Images of 10-DPA cotton bolls from WT and *GhFAD3-4* transgenic cotton plants.

(L) Statistical analysis of cotton boll weight in (K).

(M) Image of mature fiber cells from WT and *GhFAD3-4* transgenic cotton plants.

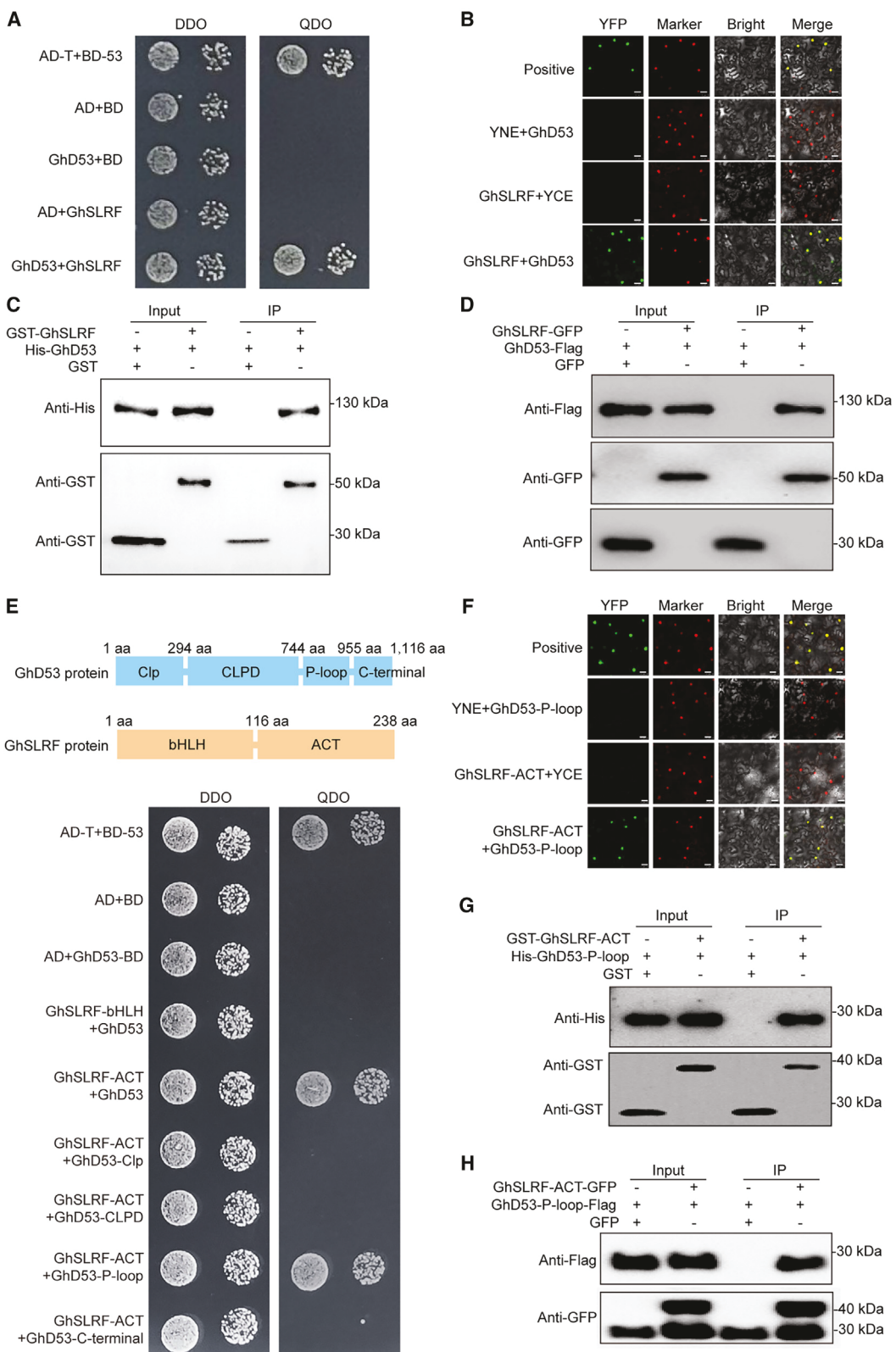
(N) Statistical analysis of fiber length in (M).

(O and P) Image of fibers of WT and *GhFAD3-4* transgenic plants treated with C18:3 or C18:3 biosynthesis inhibitor (O) and with GR24 or Tis108 (P) for 10 days.

(Q and R) Statistical analysis of fiber length in (O) and in (P), respectively.

In (A), (C), (E), (H)–(J), (L), (N), (Q), and (R), values are means \pm SD ($n = 3$ for A and J and $n = 30$ for C, E, H, I, L, N, Q, and R). *** and ** indicate $p < 0.001$ and $p < 0.01$ (Student's t test). In (B), (D), (F), (G), (K), (M), (O), and (P), scale bar, 10 mm.

See also Figure S4.



(legend on next page)

GhD53 physically interacts with transcription factor GhSLRF

D53 protein has been postulated to function as a transcriptional repressor through its interaction with other transcription factors.^{11,21,31} In this study, it was found that the transcription factor interacting with GhD53 was a basic-helix-loop-helix (bHLH) family protein, designated GhSLRF (Figures 4A and S5).

Further validation through *in vivo* bimolecular fluorescence complementation (BiFC) and coimmunoprecipitation (coIP) assays, coupled with an *in vitro* pull-down assay, further confirmed the interaction between GhD53 and GhSLRF (Figures 4B–4D). Using four methods for studying protein interactions, we determined that GhD53, aside from its DNA-binding capability for direct gene transcription regulation, also possesses ability to interact with other transcriptional factors such as GhSLRF (Figures 4E–4H), enabling transmission of SL signal downstream to regulate cotton fiber development.

GhSLRF is a positive regulator of fiber cell elongation that directly binds to the promoters of GhFAD3-2 and GhFAD3-4

GhSLRF gene exhibited robust expression in cotton fibers during their elongation and secondary cell wall thickening stages (Figure S6A). To investigate GhSLRF's role in cotton, transgenic cotton plants with either overexpressed or knocked-out GhSLRF were generated (Figures 5A, 5B, and S6B–S6E). Overexpression of GhSLRF in cotton resulted in increased cotton boll weight, fiber length, plant height, initiated fiber cell number, and mature seed weight (Figures 5C–5F and S6F–S6L). Conversely, knockout of GhSLRF led to decreased cotton boll weight, fiber length, plant height, initiated fiber cell number, and mature seed weight (Figures 5C–5F and S6F–S6L). Additionally, GhSLRF-KO transgenic line treated with SL analog GR24 failed to restore its fiber length to the same extent as GR24-treated wild-type fibers. While SL biosynthesis inhibitor Tis108 did not fully inhibit fiber elongation in GhSLRF-OE transgenic line compared with wild-type plants. These results indicate that GhSLRF operates downstream of SL signal to regulate cotton fiber elongation (Figures 5G and 5H).

GhSLRF, a bHLH-type transcription factor, localized to nucleus (Figure S6M). Furthermore, we observed that GR24 treatment promoted fiber elongation in GhSLRF-OE cottons, while Tis108 treatment inhibited fiber elongation in GhSLRF-KO cottons (Figures S6N and S6O). The expression of GhSLRF was upregulated after the treatment with GR24 and

downregulated after the treatment with Tis108 (Figure S6P). This study delves into downstream targets of GhSLRF during cotton fiber development. ChIP-seq and RNA-seq of GhSLRF transgenic cotton fibers were performed, which identified 9,034 upregulated genes after GhSLRF overexpression (Figure S6Q). Among peaks identified in ChIP-seq, 6.51% (22,719 peaks) were located in promoter regions (from -2,000 to -1 bp of the start codon), corresponding to 20,651 genes (Figure S6R). Notably, GhSLRF-IP group displayed a significant signal fraction within 2,000 bp promoter region when compared with input (control) group (Figure S6S). Previous studies have reported the binding of bHLH proteins to E-box elements in target gene promoters.³ A search for enriched motifs in binding sites within genic regions also identified E-box as a significant motif (p value = 1×10^{-38}) in promoter regions of downstream genes of GhSLRF (Figure 5I). A comparison of RNA-seq and ChIP-seq data identified 2,622 genes that were both upregulated after GhSLRF overexpression and directly bound by GhSLRF (Figure 5J; Table S4). We then investigated expression of these genes during fiber development and identified 225 genes had a high expression level (FPKM > 15) during fiber elongation stage (10-DPA fiber) (Figure S6T; Table S5). KEGG term enrichment analysis suggested that GhSLRF target genes were primarily enriched in fatty acid regulation pathways (Figure 5K).

Consistently, fatty acid profile analysis identified a significant accumulation of linolenic acid in fibers of GhSLRF overexpression lines, while knockout of GhSLRF resulted in reduced linolenic acid content (Figures S6U and 5L). GhFAD3-2A and GhFAD3-4D from fatty acid-related enriched pathways also contained this E-box binding site in their promoter regions (Figures S6V and S6W). The short fiber phenotype of GhSLRF-KO plants could be rescued by exogenous C18:3, while enhanced fiber elongation observed in GhSLRF-OE plants was impaired upon treatment with C18:3 biosynthesis inhibitor carbenoxolone. These results imply that GhSLRF regulates linolenic acid to control fiber development (Figures 5M and 5N).

Given that GhFAD3-2 and GhFAD3-4 are highly expressed during fiber elongation and their transcription is regulated by SL, we explored regulatory relationship between GhSLRF and GhFAD3-2 as well as GhFAD3-4. Our investigation suggested that overexpression of GhSLRF upregulates transcripts of GhFAD3-2 and GhFAD3-4 while knocking out of GhSLRF attenuates their expression (Figures 5O and 5P). ChIP-seq analysis

Figure 4. GhD53 directly interacts with GhSLRF

(A and E) Yeast two-hybrid assays illustrate the interaction between the GhD53 protein and GhSLRF protein (A) and between the P-loop domain of GhD53 and the ACT_UUR-ACR-like (ACT) domain of GhSLRF (E). In this context, DDO denotes -Trp/-Leu double dropout medium, while QDO represents -Trp/-Leu/-His/Ade quadruple dropout medium.

(B and F) Bimolecular fluorescence complementation (BiFC) analysis displaying the interaction between GhD53 and GhSLRF (B) and between the P-loop domain of GhD53 and the ACT domain of GhSLRF (F) in tobacco leaves.

(C and G) Pull-down assays illustrating the interaction between GhD53 and GhSLRF (C) and between the P-loop domain of GhD53 and the ACT domain of GhSLRF (G) *in vitro*. His-GhD53 protein (C) or His-GhD53-P-loop protein (G) was incubated with glutathione S-transferase (GST) or GST-GhSLRF (C)/GhSLRF- ACT (G) and precipitated with GST beads. The precipitates were analyzed by immunoblotting with anti-GST and anti-His antibodies.

(D and H) CoIP analysis showing the interaction between GhD53 and GhSLRF (D) and between the P-loop domain of GhD53 and the ACT domain of GhSLRF (H) using a transient expression system in tobacco leaves. Protein extract was precipitated with FLAG beads, and fusion proteins were detected by immunoblotting using anti-GFP antibodies.

In (B) and (F), scale bar, 25 μ m.

See also Figure S5.

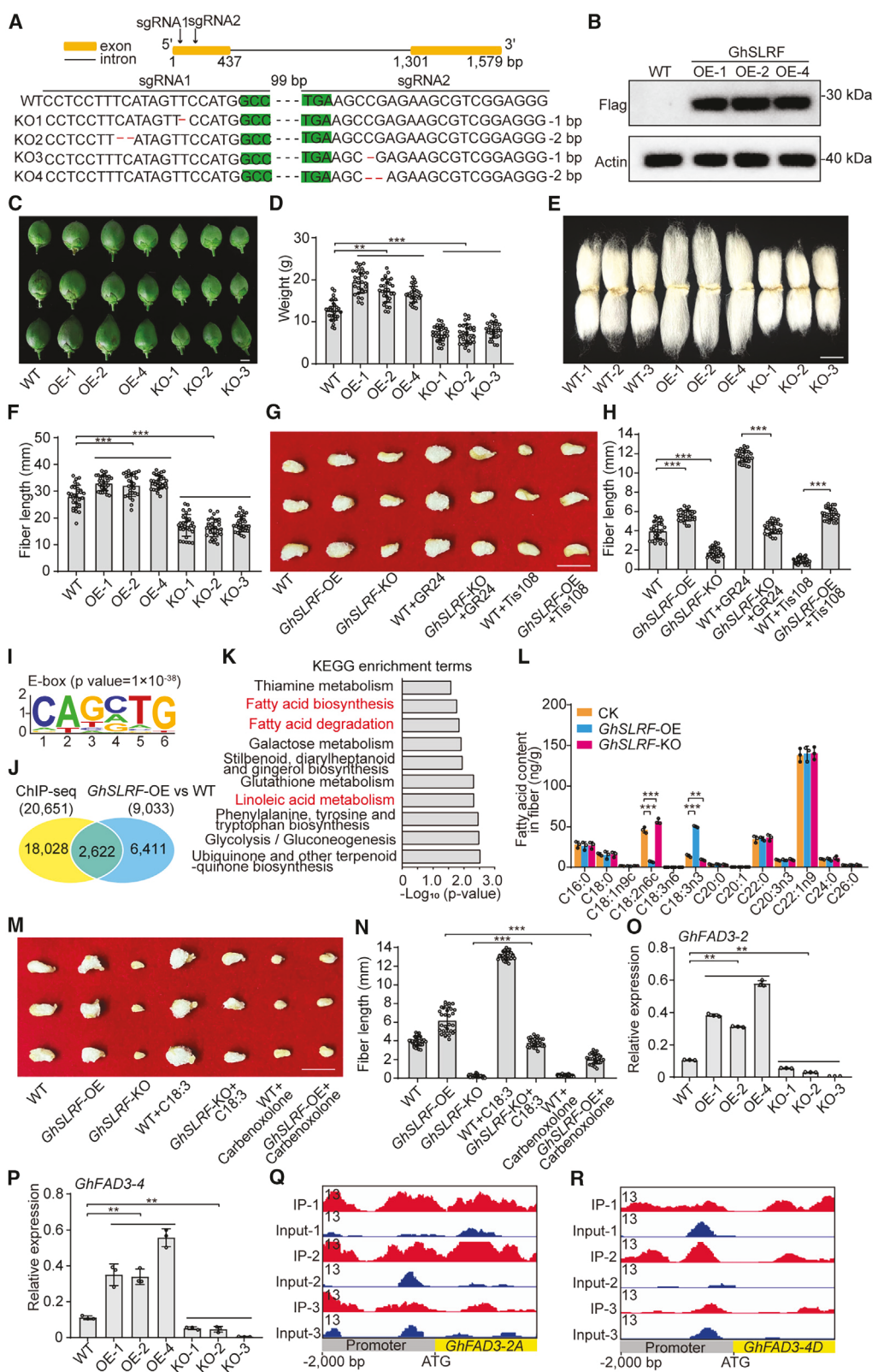


Figure 5. GhSLRF promotes fiber cell elongation in cotton

(A) Sanger sequencing-based genotyping of *GhSLRF*-knockout lines obtained through CRISPR-Cas9 gene editing. Nucleotide deletions are indicated by the red dashes.

(legend continued on next page)

demonstrated the strong binding affinity of *GhSLRF* to the promoter regions of *GhFAD3-2* and *GhFAD3-4* (Figures 5Q and 5R).

To elucidate the regulatory mechanism by which *GhSLRF* controls transcription of *GhFAD3-2* and *GhFAD3-4*, Y1H and tobacco transient assays were performed, which identified direct binding of *GhSLRF* to their respective promoters (Figures 6A–6C). Further experiments, including tobacco transient assays, dual-luciferase assays, and EMSA, identified critical *cis*-elements located within P3 or L1 fragment of *GhFAD3-2* promoter and F4 or L2 fragment of *GhFAD3-4* promoter, enabling binding of *GhSLRF* protein to these promoters (Figures 6D–6M and S7). Mutagenesis analysis underscored significance of specific binding sites for this interaction (Figures 6D–6M and S7).

GhSLRF encompasses two domains, bHLH and ACT_UUR-ACR-like (ACT). Y1H and tobacco transient assays, combined with EMSA experiments, indicated that bHLH domain of *GhSLRF*, rather than ACT domain, was responsible for physically interacting with identified *cis*-elements in P3 or L1 fragment of *GhFAD3-2* promoter and F4 or L2 fragment of *GhFAD3-4* promoter (Figures 6N–6V). ChIP assays further affirmed that *GhSLRF* is recruited and binds to *GhFAD3-2* and *GhFAD3-4* promoters (Figures 6W and 6X). These findings collectively establish that bHLH domain of *GhSLRF* confers its activity to bind to E-box *cis*-elements in *GhFAD3-2* and *GhFAD3-4* promoters, thereby activating transcription of these genes.

SL abrogates interaction between GhD53 and GhSLRF to activate GhSLRF transcriptional activity on *GhFAD3-2* and *GhFAD3-4*

Dual-luciferase assay system suggested that expression of *GhD53* led to a reduction in luciferase activity controlled by the promoters of *GhFAD3-2* and *GhFAD3-4*. Importantly, this repression effect was nullified when *GhD53*-binding sites identified in *GhFAD3-2* and *GhFAD3-4* promoters were mutated (Figures 7A and 7B). These findings suggest that *GhD53* binds to *GhFAD3-2* and *GhFAD3-4* promoters to repress their transcription.

Conversely, luciferase activity under control of *GhFAD3-2* and *GhFAD3-4* promoters was activated upon expression of *GhSLRF*. However, this activation was significantly repressed

when *GhD53* was co-expressed with *GhSLRF*, and notably, the addition of exogenous GR24 alleviated this repression effect (Figures 7C and 7D). Furthermore, mutations in *SLRF* binding sites within *GhFAD3-2* and *GhFAD3-4* promoters led to reduced luciferase activity when co-expressed with *GhSLRF*. However, application of GR24 abolished inhibitory effect of *GhD53* on *GhSLRF*-activated transcription of *GhFAD3-2* and *GhFAD3-4* (Figures 7E and 7F). Moreover, mutating D53-binding sites within *GhFAD3-2* and *GhFAD3-4* promoters abrogated inhibitory effect of *GhD53* on luciferase activity driven by native *GhFAD3-2* or *GhFAD3-4* promoters (Figures 7G and 7H). These findings collectively suggest that SL interferes in both the binding of *GhD53* to *GhFAD3* promoter and the interaction of *GhD53* with *GhSLRF*, ultimately leading to activation of *GhFAD3-2* and *GhFAD3-4* transcription.

In summary, our study identified a dual regulatory role of *GhD53* in cotton fiber development (Figure 7I). In the absence of SL, *GhD53* primarily acts as a transcription factor to directly bind to *GhFAD3-2* and *GhFAD3-4* promoters, thereby suppressing their transcription. Additionally, *GhD53* functions as an interaction factor with transcriptional activator *GhSLRF*, blocking binding and transcriptional activation of *GhSLRF* on *GhFAD3-2* and *GhFAD3-4*. This dual regulatory mechanism of *GhD53* inhibits linolenic acid biosynthesis in fibers, ultimately resulting in production of shorter fibers. By contrast, in presence of SL, *GhD53* protein is degraded, abolishing its transcriptional repression of *GhFAD3-2* and *GhFAD3-4* and simultaneously releasing transcriptional activity of its interaction partner *GhSLRF* to activate *GhFAD3-2* and *GhFAD3-4* expression. This enhances linolenic acid biosynthesis in fibers, promoting fiber elongation.

DISCUSSION

SL is an essential phytohormones governing various aspects of plant development, such as shoot branching and adventitious root development. However, most of those studies have been from the macro-phenotypic perspective, and their involvement in plant cell development at single-cell level is still not well understood. Furthermore, our comprehension of SL-mediated signaling pathways lags behind our knowledge of biosynthetic routes—for instance, the exact molecular mechanisms

(B) Western blot analysis of *GhSLRF* protein in WT and *GhSLRF*-OE transgenic cotton plants.

(C and E) Images of 10-DPA cotton bolls (C) and mature fiber cells (E) from WT and *GhSLRF* transgenic cotton plants.

(D and F) Statistical analysis of cotton boll weight (D) in (C) and fiber length (F) in (E).

(G) Image of fibers of WT and *GhSLRF* transgenic plants treated with GR24 or Tis108 for 10 days.

(H) Statistical analysis of fiber length in (G).

(I) Identification of potential *GhSLRF* binding motif with 1 kb flanking sequences around each bound peak. The number of binding region peaks (peak count frequency) corresponds to the indicated region.

(J) Venn diagram showing the extent of overlap between genes identified from ChIP-seq and RNA-seq.

(K) KEGG enrichment analysis of 225 genes upregulated in fiber elongation stage.

(L) Fatty acid content in 10-DPA fibers from WT and *GhSLRF* transgenic cotton plants.

(M) Fiber images from WT and *GhSLRF* transgenic plants after treatment with C18:3 or C18:3 inhibitor for 10 days.

(N) Statistical analysis of fiber length in (M).

(O and P) Relative expression level of *GhFAD3-2* (O) and *GhFAD3-4* (P) in fibers from WT and *GhSLRF* transgenic cotton plants.

(Q and R) Integrative Genomics Viewer (IGV) images showing binding peaks of *GhD53* in *GhFAD3-2* (Q) or *GhFAD3-4* (R) promoter. IGV 2.12.0 is used for visualizing binding peaks.

In (D), (F), (H), (L), (N), (O), and (P), values are means \pm SD ($n = 30$ for D, F, H, and N and $n = 3$ for L, O, and P). *** and ** indicate $p < 0.001$ and $p < 0.01$ (Student's t test). In (C), (E), (G), and (M), scale bar, 10 mm.

See also Figure S6 and Tables S4 and S5.

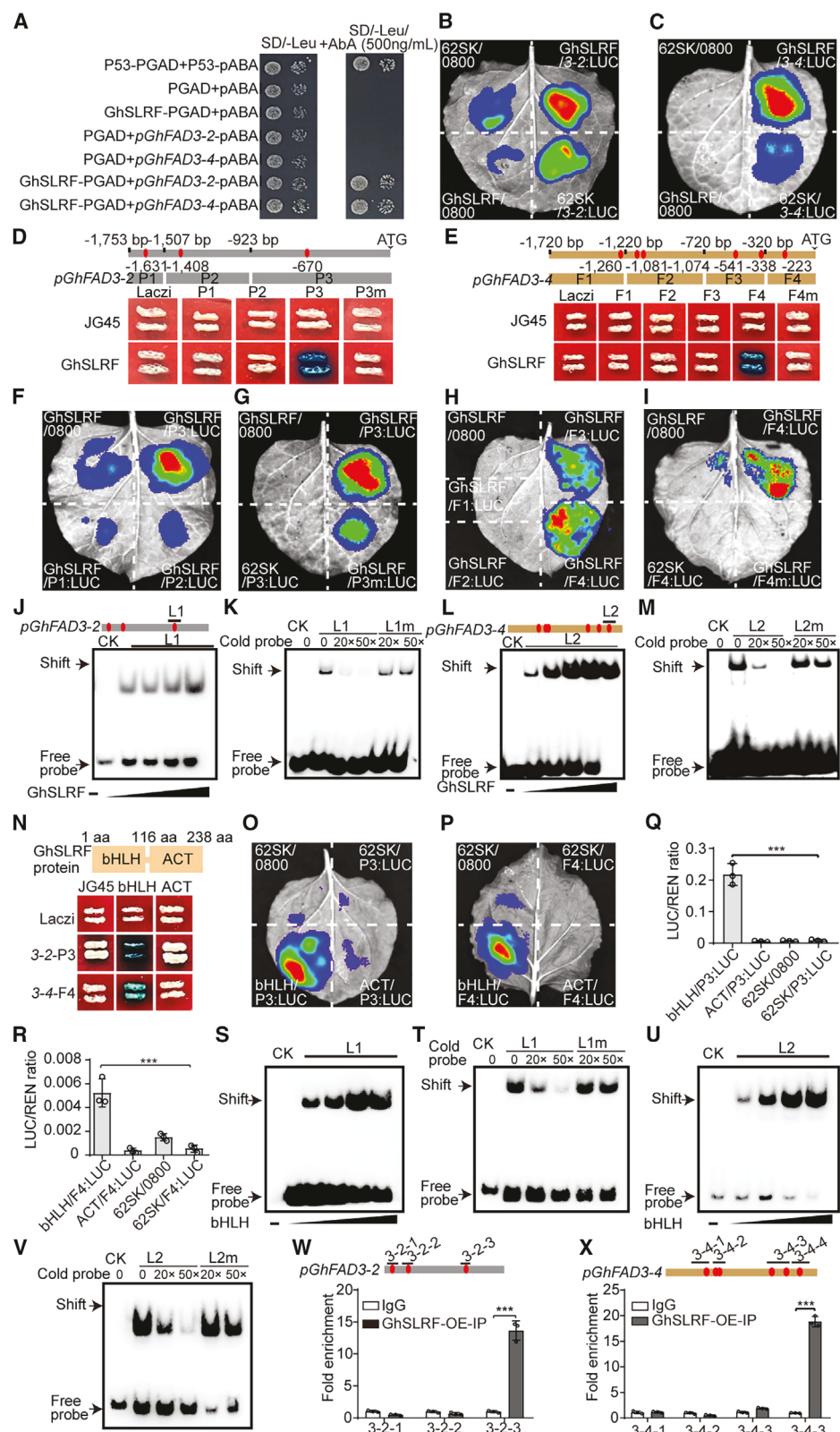


Figure 6. GhSLRF protein directly binds to promoters of *GhFAD3-2* and *GhFAD3-4*

(A) Yeast one-hybrid assay showing the binding of GhSLRF to *GhFAD3-2* and *GhFAD3-4* promoters.
(B and C) Tobacco transient expression assay of GhSLRF and *GhFAD3-2* (B) or *GhFAD3-4* (C) promoter.

(legend continued on next page)

Developmental Cell

Article



underlying SL-regulated transcriptional control by D53 have been the subject of ongoing debate.

Prior studies have shown that SL promotes fiber cell elongation, with SL content observed to increase in fibers at the elongation stage.²⁶ In this study, we demonstrated that GhD53 represses SL signal to inhibit fiber cell elongation in cotton (Figure 7i). According to previous research, the suitable concentration of GR24 is 15 μ M.²⁶ We applied the previous concentration, and the results are basically consistent with the previous report.

It was well-established that D53 physical interacts with transcription factors to inhibit the transcription of genes responsive to SL. For example, the D53 homologs in *Arabidopsis*, SMXL6/7/8, interact with SPL9 and SPL15 to repress the transcription activation activity of SPL9/SPL15 on BRC1 expression, consequently promoting branching.³² Similarly, in rice, D53 is able to interact with a key plant architecture regulator, IPA1, thereby suppressing IPA1's transcriptional activation activity and, in turn, regulating tiller number and SL-induced gene expression.²¹ Additionally, recent research has remarkably identified that D53/SMXLs can function as transcription factors to directly bind and repress target gene expression, which is exemplified by the finding that SMXL6 and SMXL7 directly bind to the promoters of SMXL6/7/8, thus negatively regulating their expression.⁹ Wang et al. provided evidence that BES1, a positive regulator in the BR signaling pathway, is one of the direct targets of MAX2 for degradation.³³ In addition, SL has been found to influence cytokinin levels by promoting the degradation of cytokinin through the transcriptional activation of CYTOKININ OXIDASE/DEHYDROGENASE 9 in rice.³⁴ This interaction underscores the interplay between SL and cytokinin. Furthermore, in *Arabidopsis*, SL has been shown to modulate polar auxin transport through the endocytosis of PIN-FORMED1 (PIN1).³⁵ In rice, basipetal polar auxin transport is elevated in the *d27* mutant, and the indole-3-acetic acid (IAA) level is increased in the *d3* mutant,³⁶ emphasizing the importance of crosstalk between SL and auxin in both species. Considering these prior findings, a comprehensive investigation of the potential regulation of SL-inducible genes *GhFAD3* and *GhSLRF* by other phytohormones is warranted.

Unfortunately, due to technical reasons, when studying the function of *GhFAD3-2*, only *GhFAD3-2*-RNAi materials were obtained, and no *GhFAD3-2*-KO materials were obtained.

Enhancing cotton fiber quality without compromising yield is a formidable challenge for cotton breeders. Nevertheless, our research has demonstrated the feasibility of simultaneously improving both cotton fiber quality and yield. Our research contributes to this understanding by identifying genes that positively regulate both fiber yield and seed yield. Fiber cells originate from the epidermal cells of cotton seeds. Studies by Ruan³⁷, Zeng et al.³⁸, Pugh et al.³⁹, Xu et al.⁴⁰, Zhao et al.⁴¹, Mukherjee et al.⁴², and Ding et al.⁴³ have all highlighted the positive correlation between fiber yield and seed yield in cotton.^{3,34,37} Our findings align with these studies and highlight the potential of genes such as GhD53, GhFAD3-2, and GhSLRK as promising candidates for improving both fiber and seed yield in cotton.

Our study not only deepens our fundamental knowledge of plant development but also offers tangible benefits for cotton agriculture and industry. It highlights the potential for targeted genetic interventions to enhance cotton fiber quality and yield, contributing to the sustainability and competitiveness of the cotton sector.

Limitations of the study

In this study, we used *GhFAD3-2*-RNAi and *GhD53*-RNAi materials instead of knockout material for the determination of the function of *GhFAD3-2* and *GhD53*. In this study, the fiber phenotypes of various transgenic materials were obtained from the planting materials in the laboratory, and the corresponding fiber phenotypes were not obtained from large-scale planting materials in the field. These are limitations of this study.

RESOURCE AVAILABILITY

Lead contact

Further information and requests for resources and reagents should be directed to and will be fulfilled by the lead contact, Guanghui Xiao (guanghuix@snnu.edu.cn).

(D and E) Yeast one-hybrid assay showing the binding of GhSLRF to different fragments of *GhFAD3-2* promoter (D) and *GhFAD3-4* promoter (E). The red ovals represent the GhSLRF binding sites.

(F–I) Tobacco transient expression assay of GhSLRF and *GhFAD3-2* promoter fragments with native (F) or mutated (G) binding site, of GhSLRF and *GhFAD3-4* promoter fragments with intact (H) or mutated (I) binding site.

(J and L) EMSA demonstrating GhSLRF's direct binding to the L1 fragment of the *GhFAD3-2* promoter (J) and the L2 fragment of the *GhFAD3-4* promoter (L).

(K and M) Competitive EMSA assay using a biotin-labeled L1 fragment of the *GhFAD3-2* promoter (K) and a biotin-labeled L2 fragment of the *GhFAD3-4* promoter (M) incubated with GhD53, competing with different concentrations of cold probes (without biotin label) containing the intact or mutated binding site (L1m, K or L2m, M).

(N) Yeast one-hybrid assay demonstrating the binding of two domains of GhSLRF to the P3 fragment of the *GhFAD3-2* promoter and the F4 fragment of the *GhFAD3-4* promoter.

(O and P) Tobacco transient expression assay identifying the interaction of GhSLRF's bHLH domain with the *GhFAD3-2*-P3 promoter fragment (O) and the *GhFAD3-4*-F4 promoter fragment (P).

(Q and R) Statistical analysis of luminescence intensity in (O) and (P), respectively.

(S and U) EMSA assay showing that GhSLRF's bHLH domain directly binds to the L1 fragment of *GhFAD3-2* promoter (S) and the L2 fragment of *GhFAD3-4* promoter (U).

(T and V) Competitive EMSA assay using a biotin-labeled L1 fragment of the *GhFAD3-2* promoter (T) and a biotin-labeled L2 fragment of the *GhFAD3-4* promoter (V) incubated with the bHLH domain, competing with different concentrations of cold probes (without biotin label) of intact or mutated binding site (L1m, T and L2m, V).

(W and X) ChIP-qPCR analysis showing a high degree of enrichment in the 3-2-3 region of *GhFAD3-2* promoter (W) and 3-4-4 region of *GhFAD3-4* promoter (X) in GhSLRF-OE lines.

In (Q), (R), (W), and (X), values are means \pm SD ($n = 3$). *** indicates $p < 0.001$ (Student's t test).

See also Figure S7.

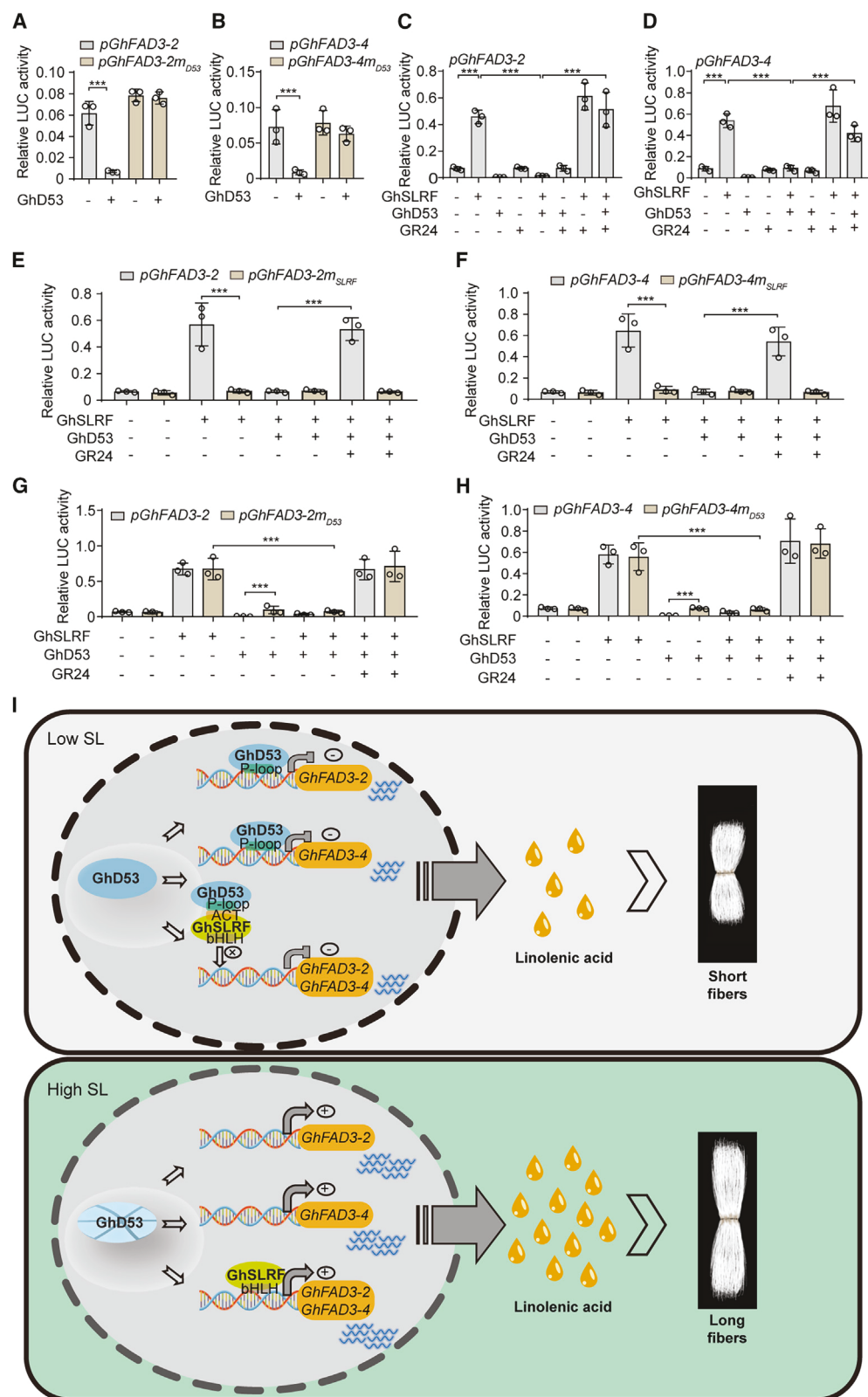


Figure 7. SL alleviates GhD53's inhibitory effect on GhSLRF activation of downstream GhFAD3-2 and GhFAD3-4 gene transcription

(A and B) Relative luciferase (LUC) activities of *GhFAD3-2* (A) or *GhFAD3-4* (B) promoter with or without D53-binding site when co-transformed with GhD53 protein. Relative LUC activities were normalized to the REN (*Renilla luciferase*) internal control.

(legend continued on next page)

Developmental Cell

Article



Materials availability

All data required to support the claims of this paper are included in the main and [supplemental information](#).

All reagents generated in this study are available on request from the [lead contact](#).

Data and code availability

RNA-seq data of fibers treated with GR24 or Tis108 are stored in the biological project library of NCBI with accession number PRJNA871199. The RNA-seq data of *GhD53* and *GhSLRF* transgenic cotton fibers are available at NCBI with accession number PRJNA1015026. The ChIP-seq data of 5 DPA fibers from *GhD53* and *GhSLRF* transgenic cottons are available at NCBI with accession number PRJNA1014915. The DAP-seq data of *GhD53* protein is available at NCBI with accession number PRJNA1029020.

All data required to substantiate the claims of this paper are included in main or [supplemental information](#).

This paper does not report original code.

Any additional information required to reanalyze the data reported in this paper is available from the [lead contact](#) upon request.

ACKNOWLEDGMENTS

We thank Dr. Yuxian Zhu (The Institute for Advanced Studies, Wuhan University) and Bing Wang (Institute of Genetics and Departmental Biology, Chinese Academy of Sciences) for assistance. This work was supported by the National Key Research and Development Program of China (2022YFF1002000 to G.X.), the National Natural Science Foundation of China (32070549 to G.X., 32270578 to G.X., 32200444 to L.Z., and 32300433 to H.W.), the Hong Kong Scholars Program (XJ2023014 to L.Z.), the Key Science and Technology Research Program of Xinjiang Province (KC00310501 to G.X.), and the U.S. National Science Foundation (grant no. 2238942 to L.L.).

AUTHOR CONTRIBUTIONS

H.W., M.F., S.W., X.Z., H.Z., Y.S., J.C., L.H., and M.H. performed the experiments. H.W., L.Z., and M.F. analyzed the data. L.Z., R.T., L.L., and G.X. wrote and revised the paper.

DECLARATION OF INTERESTS

The authors declare no competing interests.

STAR METHODS

Detailed methods are provided in the online version of this paper and include the following:

- [KEY RESOURCES TABLE](#)
- [EXPERIMENTAL MODEL AND STUDY PARTICIPANT DETAILS](#)
 - Plant material and growth conditions
- [METHOD DETAILS](#)
 - Cotton transformation
 - Cotton ovule culture

(C and D) Relative LUC activities of *GhFAD3-2* (C) or *GhFAD3-4* (D) promoter when co-transformed with *GhSLRF* and *GhD53* protein with or without GR24 treatment.

(E and F) Relative LUC activities of *GhFAD3-2* (E) or *GhFAD3-4* (F) promoter with or without SLRF binding site when co-transformed with *GhSLRF* and *GhD53* protein with or without GR24 treatment.

(G and H) Relative LUC activities of *GhFAD3-2* (G) or *GhFAD3-4* (H) promoter with or without D53-binding site when co-transformed with *GhSLRF* and *GhD53* protein with or without GR24 treatment.

(I) A schematic diagram illustrates the mechanistic framework of *GhD53* in regulating cotton fiber cell elongation. In the absence of SL, *GhD53* directly inhibits the transcription of *GhFAD3-2* and *GhFAD3-4*. Additionally, the P-loop domain of *GhD53* interacts with the ACT domain of *GhSLRF*, resulting in the transcriptional inhibition of *GhFAD3-2* and *GhFAD3-4*. This dual inhibition leads to reduced linolenic acid accumulation and shorter cotton fiber. Conversely, when SL is present, the *GhD53* protein undergoes degradation. Consequently, this degradation removes *GhD53*-mediated transcriptional inhibition of *GhFAD3-2* and *GhFAD3-4*. Simultaneously, it releases *GhSLRF* protein, which further promotes the transcription of *GhFAD3-2* and *GhFAD3-4*. This coordinated action results in increased linolenic acid content and longer cotton fiber.

In (A–H), values are means \pm SD ($n = 3$). Values are means \pm SD ($n = 3$). *** indicates $p < 0.001$ (Student's t test).

- RNA extraction and RT-qPCR analysis
- Protein extraction and western blot
- ChIP-seq and ChIP-qPCR
- DAP-seq assay
- Subcellular location
- Yeast one-hybrid assay
- Dual-luciferase (Dual-LUC) reporter assay
- Electrophoretic mobility shift assay (EMSA)
- Yeast two-hybrid assay
- BiFC assay
- Co-IP assay
- Pull-down assay
- RNA-seq analyses
- Fatty acid content detection
- Microscopic analysis
- Phylogenetic, sequence alignment and domain analysis

● [QUANTIFICATION AND STATISTICAL ANALYSIS](#)

SUPPLEMENTAL INFORMATION

Supplemental information can be found online at <https://doi.org/10.1016/j.devcel.2024.12.009>.

Received: December 20, 2023

Revised: June 6, 2024

Accepted: December 4, 2024

Published: December 27, 2024

REFERENCES

1. Pacifici, E., Di Mambro, R., Dello Iorio, R., Costantino, P., and Sabatini, S. (2018). Acidic cell elongation drives cell differentiation in the *Arabidopsis* root. *EMBO J.* 37, e99134. <https://doi.org/10.1525/embj.201899134>.
2. Haruta, M., Sabat, G., Stecker, K., Minkoff, B.B., and Sussman, M.R. (2014). A peptide hormone and its receptor protein kinase regulate plant cell expansion. *Science* 343, 408–411. <https://doi.org/10.1126/science.1244454>.
3. Zhu, L., Wang, H., Zhu, J., Wang, X., Jiang, B., Hou, L., and Xiao, G. (2023). A conserved brassinosteroid-mediated BES1-CERP-EXPA3 signaling cascade controls plant cell elongation. *Cell Rep.* 42, 112301. <https://doi.org/10.1016/j.celrep.2023.112301>.
4. Huang, G., Huang, J.Q., Chen, X.Y., and Zhu, Y.X. (2021). Recent advances and future perspectives in cotton research. *Annu. Rev. Plant Biol.* 72, 437–462. <https://doi.org/10.1146/annurev-arplant-080720-113241>.
5. Lee, J.J., Woodward, A.W., and Chen, Z.J. (2007). Gene expression changes and early events in cotton fibre development. *Ann. Bot.* 100, 1391–1401. <https://doi.org/10.1093/aob/mcm232>.
6. Gou, J.Y., Wang, L.J., Chen, S.P., Hu, W.L., and Chen, X.Y. (2007). Gene expression and metabolite profiles of cotton fiber during cell elongation and secondary cell wall synthesis. *Cell Res.* 17, 422–434. <https://doi.org/10.1038/sj.cr.7310150>.

7. Nakano, M., Omae, N., and Tsuda, K. (2022). Inter-organismal phytohormone networks in plant-microbe interactions. *Curr. Opin. Plant Biol.* 68, 102258. <https://doi.org/10.1016/j.pbi.2022.102258>.
8. Cook, C.E., Whichard, L.P., Turner, B., Wall, M.E., and Egley, G.H. (1966). Germination of Witchweed (*Striga lutea* Lour.): isolation and properties of a potent stimulant. *Science* 154, 1189–1190. <https://doi.org/10.1126/science.154.3753.1189>.
9. Wang, L., Wang, B., Yu, H., Guo, H., Lin, T., Kou, L., Wang, A., Shao, N., Ma, H., Xiong, G., et al. (2020). Transcriptional regulation of strigolactone signalling in Arabidopsis. *Nature* 583, 277–281. <https://doi.org/10.1038/s41586-020-2382-x>.
10. Al-Babili, S., and Bouwmeester, H.J. (2015). Strigolactones, a novel carotenoid-derived plant hormone. *Annu. Rev. Plant Biol.* 66, 161–186. <https://doi.org/10.1146/annurev-arplant-043014-114759>.
11. Waters, M.T., Gutjahr, C., Bennett, T., and Nelson, D.C. (2017). Strigolactone signaling and evolution. *Annu. Rev. Plant Biol.* 68, 291–322. <https://doi.org/10.1146/annurev-arplant-042916-040925>.
12. Gomez-Roldan, V., Femas, S., Brewer, P.B., Puech-Pagès, V., Dun, E.A., Pillot, J.P., Letisse, F., Matusova, R., Danoun, S., Portais, J.C., et al. (2008). Strigolactone inhibition of shoot branching. *Nature* 455, 189–194. <https://doi.org/10.1038/nature07271>.
13. An, J., Zhao, L., Cao, Y., Ai, D., Li, M., You, C., and Han, Y. (2024). The SMXL8-AGL9 module mediates crosstalk between strigolactone and gibberellin to regulate strigolactone-induced anthocyanin biosynthesis in apple. *Plant Cell* 25. <https://doi.org/10.1093/plcell/koae191>.
14. Li, X., Lu, J., Zhu, X., Dong, Y., Liu, Y., Chu, S., Xiong, E., Zheng, X., and Jiao, Y. (2023). AtMYBS1 negatively regulates heat tolerance by directly repressing the expression of max1 required for strigolactone biosynthesis in Arabidopsis. *Plant Commun.* 4, 100675. <https://doi.org/10.1016/j.xplc.2023.100675>.
15. Wang, X., Li, Z., Shi, Y., Liu, Z., Zhang, X., Gong, Z., and Yang, S. (2023). Strigolactones promote plant freezing tolerance by releasing the WRKY41-mediated inhibition of CBF/DREB1 expression. *EMBO J.* 42, e112999. <https://doi.org/10.15252/embj.2022112999>.
16. Alder, A., Jamil, M., Marzorati, M., Bruno, M., Vermathen, M., Bigler, P., Ghislia, S., Bouwmeester, H., Beyer, P., and Al-Babili, S. (2012). The path from beta-carotene to carlactone, a strigolactone-like plant hormone. *Science* 335, 1348–1351. <https://doi.org/10.1126/science.1218094>.
17. Seto, Y., Sado, A., Asami, K., Hanada, A., Umehara, M., Akiyama, K., and Yamaguchi, S. (2014). Carlactone is an endogenous biosynthetic precursor for strigolactones. *Proc. Natl. Acad. Sci. USA* 111, 1640–1645. <https://doi.org/10.1073/pnas.1314805111>.
18. Shabek, N., Ticchiarelli, F., Mao, H., Hinds, T.R., Leyser, O., and Zheng, N. (2018). Structural plasticity of D3-D14 ubiquitin ligase in strigolactone signalling. *Nature* 563, 652–656. <https://doi.org/10.1038/s41586-018-0743-5>.
19. Ma, H., Duan, J., Ke, J., He, Y., Gu, X., Xu, T.H., Yu, H., Wang, Y., Brunzelle, J.S., Jiang, Y., et al. (2017). A D53 repression motif induces oligomerization of TOPLESS corepressors and promotes assembly of a corepressor-nucleosome complex. *Sci. Adv.* 3, e1601217. <https://doi.org/10.1126/sciadv.1601217>.
20. Zhou, F., Lin, Q., Zhu, L., Ren, Y., Zhou, K., Shabek, N., Wu, F., Mao, H., Dong, W., Gan, L., et al. (2013). D14-SCF(D3)-dependent degradation of D53 regulates strigolactone signalling. *Nature* 504, 406–410. <https://doi.org/10.1038/nature12878>.
21. Song, X., Lu, Z., Yu, H., Shao, G., Xiong, J., Meng, X., Jing, Y., Liu, G., Xiong, G., Duan, J., et al. (2017). IPA1 functions as a downstream transcription factor repressed by D53 in strigolactone signalling in rice. *Cell Res.* 27, 1128–1141. <https://doi.org/10.1038/cr.2017.102>.
22. Liang, Y., Ward, S., Li, P., Bennett, T., and Leyser, O. (2016). SMXL1-LIKE7 signals from the nucleus to regulate shoot development in Arabidopsis via partially EAR motif-independent mechanisms. *Plant Cell* 28, 1581–1601. <https://doi.org/10.1105/tpc.16.00286>.
23. Wang, L., Wang, B., Jiang, L., Liu, X., Li, X., Lu, Z., Meng, X., Wang, Y., Smith, S.M., and Li, J. (2015). Strigolactone signaling in Arabidopsis regulates shoot development by targeting D53-Like SMXL repressor proteins for ubiquitination and degradation. *Plant Cell* 27, 3128–3142. <https://doi.org/10.1105/tpc.15.00605>.
24. Soundappan, I., Bennett, T., Morffy, N., Liang, Y., Stanga, J.P., Abbas, A., Leyser, O., and Nelson, D.C. (2015). SMXL1-LIKE/D53 family members enable distinct max2-dependent responses to strigolactones and karrikins in Arabidopsis. *Plant Cell* 27, 3143–3159. <https://doi.org/10.1105/tpc.15.00562>.
25. Kapulnik, Y., Resnick, N., Mayzlish-Gati, E., Kaplan, Y., Wininger, S., Hershenhorn, J., and Koltai, H. (2011). Strigolactones interact with ethylene and auxin in regulating root-hair elongation in Arabidopsis. *J. Exp. Bot.* 62, 2915–2924. <https://doi.org/10.1093/jxb/erq464>.
26. Tian, Z., Zhang, Y., Zhu, L., Jiang, B., Wang, H., Gao, R., Friml, J., and Xiao, G. (2022). Strigolactones act downstream of gibberellins to regulate fiber cell elongation and cell wall thickness in cotton (*Gossypium hirsutum*). *Plant Cell* 34, 4816–4839. <https://doi.org/10.1093/plcell/koac270>.
27. Sun, Y., Tian, Z., Zuo, D., Cheng, H., Wang, Q., Zhang, Y., Lv, L., and Song, G. (2024). Strigolactone-induced degradation of SUPPRESSOR OF MORE AXILLARY GROWTH2-LIKE7 (SMXL7) and SMXL8 contributes to gibberellin- and auxin-mediated fiber cell elongation in cotton. *Plant Cell* 36, 3875–3893. <https://doi.org/10.1093/plcell/koae212>.
28. de Saint Germain, A., Ligerot, Y., Dun, E.A., Pillot, J.P., Ross, J.J., Beveridge, C.A., and Rameau, C. (2013). Strigolactones stimulate internode elongation independently of gibberellins. *Plant Physiol.* 163, 1012–1025. <https://doi.org/10.1104/pp.113.220541>.
29. Ito, S., Braguy, J., Wang, J.Y., Yoda, A., Fiorilli, V., Takahashi, I., Jamil, M., Felemban, A., Miyazaki, S., Mazzarella, T., et al. (2022). Canonical strigolactones are not the major determinant of tillering but important rhizospheric signals in rice. *Sci. Adv.* 8, eadd1278. <https://doi.org/10.1126/sciadv.add1278>.
30. Mendes, A., Kelly, A.A., van Erp, H., Shaw, E., Powers, S.J., Kurup, S., and Eastmond, P.J. (2013). bZIP67 regulates the omega-3 fatty acid content of Arabidopsis seed oil by activating fatty acid desaturase 3. *Plant Cell* 25, 3104–3116. <https://doi.org/10.1105/tpc.113.116343>.
31. Bürger, M. (2021). Insights into the evolution of strigolactone signaling. *Plant Cell* 33, 3389–3390. <https://doi.org/10.1093/plcell/koab216>.
32. Xie, Y., Liu, Y., Ma, M., Zhou, Q., Zhao, Y., Zhao, B., Wang, B., Wei, H., and Wang, H. (2020). Arabidopsis FHY3 and FAR1 integrate light and strigolactone signaling to regulate branching. *Nat. Commun.* 11, 1955. <https://doi.org/10.1038/s41467-020-15893-7>.
33. Wang, Y., Sun, S., Zhu, W., Jia, K., Yang, H., and Wang, X. (2013). Strigolactone/MAX2-induced degradation of brassinosteroid transcriptional effector BES1 regulates shoot branching. *Dev. Cell* 27, 681–688. <https://doi.org/10.1016/j.devcel.2013.11.010>.
34. Duan, J., Yu, H., Yuan, K., Liao, Z., Meng, X., Jing, Y., Liu, G., Chu, J., and Li, J. (2019). Strigolactone promotes cytokinin degradation through transcriptional activation of CYTOKININ OXIDASE/DEHYDROGENASE 9 in rice. *Proc. Natl. Acad. Sci. USA* 116, 14319–14324. <https://doi.org/10.1073/pnas.1810980116>.
35. van Rongen, M., Bennett, T., Ticchiarelli, F., and Leyser, O. (2019). Connective auxin transport contributes to strigolactone-mediated shoot branching control independent of the transcription factor BRC1. *PLOS Genet.* 15, e1008023. <https://doi.org/10.1371/journal.pgen.1008023>.
36. Sun, H., Tao, J., Hou, M., Huang, S., Chen, S., Liang, Z., Xie, T., Wei, Y., Xie, X., Yoneyama, K., et al. (2015). A strigolactone signal is required for adventitious root formation in rice. *Ann. Bot.* 115, 1155–1162. <https://doi.org/10.1093/aob/mcv052>.
37. Ruan, Y.L. (2013). Boosting seed development as a new strategy to increase cotton fiber yield and quality. *J. Integr. Plant Biol.* 55, 572–575. <https://doi.org/10.1111/jipb.12074>.
38. Zeng, J., Yan, X., Bai, W., Zhang, M., Chen, Y., Li, X., Hou, L., Zhao, J., Ding, X., Liu, R., et al. (2022). Carpel-specific down-regulation of

Developmental Cell

Article



GhCKXs in cotton significantly enhances seed and fiber yield. *J. Exp. Bot.* 73, 6758–6772. <https://doi.org/10.1093/jxb/erac303>.

39. Pugh, D.A., Offler, C.E., Talbot, M.J., and Ruan, Y.L. (2010). Evidence for the role of transfer cells in the evolutionary increase in seed and fiber biomass yield in cotton. *Mol. Plant* 3, 1075–1086. <https://doi.org/10.1093/mp/ssq054>.

40. Xu, S.M., Brill, E., Llewellyn, D.J., Furbank, R.T., and Ruan, Y.L. (2012). Overexpression of a potato sucrose synthase gene in cotton accelerates leaf expansion, reduces seed abortion, and enhances fiber production. *Mol. Plant* 5, 430–441. <https://doi.org/10.1093/mp/ssr090>.

41. Zhao, J., Bai, W., Zeng, Q., Song, S., Zhang, M., Li, X., Hou, L., Xiao, Y., Luo, M., Li, D., et al. (2015). Moderately enhancing cytokinin level by down-regulation of GhCKX expression in cotton concurrently increases fiber and seed yield. *Mol. Breed.* 35, 60. <https://doi.org/10.1007/s11032-015-0232-6>.

42. Mukherjee, T., Ivanova, M., Dagda, M., Kanayama, Y., Granot, D., and Holaday, A.S. (2015). Constitutively overexpressing a tomato fructokinase gene (LeFRK1) in cotton (*Gossypium hirsutum* L. cv. Coker 312) positively affects plant vegetative growth, boll number and seed cotton yield. *Funct. Plant Biol.* 42, 899–908. <https://doi.org/10.1071/FP15035>.

43. Ding, X., Zeng, J., Huang, L., Li, X., Song, S., and Pei, Y. (2019). Senescence-induced expression of ZmSUT1 in cotton delays leaf senescence while the seed coat-specific expression increases yield. *Plant Cell Rep.* 38, 991–1000. <https://doi.org/10.1007/s00299-019-02421-1>.

44. Ge, X., Xu, J., Yang, Z., Yang, X., Wang, Y., Chen, Y., Wang, P., and Li, F. (2023). Efficient genotype-independent cotton genetic transformation and genome editing. *J. Integr. Plant Biol.* 65, 907–917. <https://doi.org/10.1111/jipb.13427>.

45. Zhu, L., Dou, L., Shang, H., Li, H., Yu, J., and Xiao, G. (2021). GhPIPLC2D promotes cotton fiber elongation by enhancing ethylene biosynthesis. *iScience.* *iScience* 24, 102199. <https://doi.org/10.1016/j.isci.2021.102199>.

46. Bradford, M.M. (1976). A rapid and sensitive method for the quantitation of microgram quantities of protein utilizing the principle of protein-dye binding. *Anal. Biochem.* 72, 248–254. [https://doi.org/10.1016/0003-2697\(76\)90527-3](https://doi.org/10.1016/0003-2697(76)90527-3).

47. Duan, E., Wang, Y., Li, X., Lin, Q., Zhang, T., Wang, Y., Zhou, C., Zhang, H., Jiang, L., Wang, J., et al. (2019). OsSHI1 regulates plant architecture through modulating the transcriptional activity of IPA1 in rice. *Plant Cell* 31, 1026–1042. <https://doi.org/10.1105/tpc.19.00023>.

48. Saleh, A., Alvarez-Venegas, R., and Avramova, Z. (2008). An efficient chromatin immunoprecipitation (ChIP) protocol for studying histone modifications in *Arabidopsis* plants. *Nat. Protoc.* 3, 1018–1025. <https://doi.org/10.1038/nprot.2008.66>.

49. Love, M.I., Huber, W., and Anders, S. (2014). Moderated estimation of fold change and dispersion for RNA-seq data with DESeq2. *Genome Biol.* 15, 550. <https://doi.org/10.1186/s13059-014-0550-8>.

50. Liu, G.J., Xiao, G.H., Liu, N.J., Liu, D., Chen, P.S., Qin, Y.M., and Zhu, Y.X. (2015). Targeted lipidomics studies reveal that linolenic acid promotes cotton fiber elongation by activating phosphatidylinositol and phosphatidylinositol monophosphate biosynthesis. *Mol. Plant* 8, 911–921. <https://doi.org/10.1016/j.molp.2015.02.010>.

51. Hung, J.H., and Weng, Z. (2016). Sequence alignment and homology search with BLAST and ClustalW. *Cold Spring Harb. Protoc.* 2016. <https://doi.org/10.1101/pdb.prot093088>.

52. Hall, T.A. (1999). BioEdit: A user-friendly biological sequence alignment editor and analysis program for windows 95/98/NT. *Nucleic Acids Symposium Series* 41, 95–98. https://doi.org/10.14601/phytopathol_mediterr-14998u1.29.

STAR★METHODS

KEY RESOURCES TABLE

REAGENT or RESOURCE	SOURCE	IDENTIFIER
Antibodies		
Mouse monoclonal anti-GFP	Sangon Biotech	Cat#: D191040-0100
Mouse monoclonal anti-Flag	Sangon Biotech	Cat#: D191041-0100
Mouse monoclonal anti-GST	Sangon Biotech	Cat#: D190101-0200
Mouse monoclonal anti-His	Sangon Biotech	Cat#: D191001-0100
Mouse monoclonal anti-actin	Sangon Biotech	Cat#: D191048-0050
HRP-conjugated anti-mouse secondary antibody	Sangon Biotech	Cat#: D110098-0100
Bacterial and virus strains		
<i>Escherichia coli</i> strain DH5a	Weidi	Cat#: DL1001
<i>Escherichia coli</i> strain BL21(DE3)	Weidi	Cat#: EC1001
<i>Agrobacterium tumefaciens</i> GV3101	Weidi	Cat#: AC1001
<i>Agrobacterium tumefaciens</i> LBA4404	Weidi	Cat#: AC1030
Chemicals, peptides, and recombinant proteins		
rac-GR24	Solarbio	Cat#: 76974-79-3
Tis108	Solarbio	Cat#: 1315459-30-3
C18:3	Solarbio	Cat#: SL8530
carbenoxolone	Solarbio	Cat#: 7421-40-1
PI	Sigma	Cat#: P4864
Glutaraldehyde	Solarbio	Cat#: P1126
ethanol	aladdin	Cat#: E130059
methanol	Sangon	Cat#: A601617
SDS	Solarbio	Cat#: S8010
AbA	Solarbio	Cat#: A6870
X-gal	Sangon	Cat#: A600083
SD/-Trp-Ura	Coolaber	Cat#: PM2260
Tris	Solarbio	Cat#: T8060
Boric acid	Sigma	Cat#: B0252
EDTA	Solarbio	Cat#: E8040
formaldehyde	Sangon	Cat#: A602292
glycine	Solarbio	Cat#: G8200
1/2 Murashige and Skoog	Coolaber	Cat#: PM1061
DAPI	Solarbio	Cat#: C0065
O.C.T. Compound	Solarbio	Cat#: 4583
calcofluor white	Sigma	Cat#: 18909
Critical commercial assays		
RNAprep Pure Plant Kit	Tiangen	Cat#: DP441
RevertAid First Strand cDNA Synthesis Kit	Thermo	Cat#: K1622
Dual-Luciferase Reporter Assay System	Promega	Cat#: E1910
ChamQ SYBR qPCR Master Mix	Vazyme	Cat#: Q311-03
HiScript II Q RT SuperMix for qPCR (+gDNA wiper)	Vazyme	Cat#: R223-01
Cellulose Content Assay Kit	Solarbio	Cat#: BC4280
Hemicellulose Content Assay Kit	Solarbio	Cat#: BC4445
Lignin Content Assay Kit	Solarbio	Cat#: BC4200

(Continued on next page)

Continued

REAGENT or RESOURCE	SOURCE	IDENTIFIER
Deposited data		
Origin full blot images	This paper; Mendeley	Mendeley Data: https://data.mendeley.com/datasets/f7ggbyrb5/1 https://doi.org/10.17632/f7ggbyrb5.1
Experimental models: Organisms/strains		
<i>Gossypium hirsutum</i> : <i>GhD53</i> -OE	This paper	N/A
<i>Gossypium hirsutum</i> : <i>GhD53</i> -RNAi	This paper	N/A
<i>Gossypium hirsutum</i> : <i>GhFAD3-2</i> -OE	This paper	N/A
<i>Gossypium hirsutum</i> : <i>GhFAD3-2</i> -RNAi	This paper	N/A
<i>Gossypium hirsutum</i> : <i>GhFAD3-4</i> -OE	This paper	N/A
<i>Gossypium hirsutum</i> : <i>GhFAD3-4</i> -Cas9	This paper	N/A
<i>Gossypium hirsutum</i> : <i>GhSLRF</i> -OE	This paper	N/A
<i>Gossypium hirsutum</i> : <i>GhSLRF</i> -Cas9	This paper	N/A
<i>Nicotiana benthamiana</i>	N/A	N/A
<i>Saccharomyces cerevisiae</i> : <i>Y1H Gold</i>	This paper	N/A
<i>Saccharomyces cerevisiae</i> : <i>EGY48</i>	Weidi	Cat#: YC1030
Recombinant DNA		
pLacZi-pGhFAD3-2-P1	This paper	N/A
pLacZi-pGhFAD3-2-P2	This paper	N/A
pLacZi-pGhFAD3-2-P3	This paper	N/A
pLacZi-pGhFAD3-2	This paper	N/A
pLacZi-pGhFAD3-4-F1	This paper	N/A
pLacZi-pGhFAD3-4-F2	This paper	N/A
pLacZi-pGhFAD3-4-F3	This paper	N/A
pLacZi-pGhFAD3-4-F4	This paper	N/A
pLacZi-pGhFAD3-4	This paper	N/A
JG45-GhD53	This paper	N/A
JG45-GhSLRF	This paper	N/A
pGADT7-GhD53	This paper	N/A
pGADT7-GhSLRF	This paper	N/A
pLacZi-pGhD53-1	This paper	N/A
pLacZi-pGhD53-2	This paper	N/A
pLacZi-pGhD53-3	This paper	N/A
pLacZi-pGhD53-4	This paper	N/A
pLacZi-pGhD53-5	This paper	N/A
pLacZi-pGhD53-6	This paper	N/A
62SK-GhD53	This paper	N/A
62SK-GhSLRF	This paper	N/A
0800-pGhFAD3-2	This paper	N/A
0800-pGhFAD3-2-P1	This paper	N/A
0800-pGhFAD3-2-P2	This paper	N/A
0800-pGhFAD3-2-P3	This paper	N/A
0800-pGhFAD3-4	This paper	N/A
0800-pGhFAD3-4-F1	This paper	N/A
0800-pGhFAD3-4-F2	This paper	N/A
0800-pGhFAD3-4-F3	This paper	N/A
0800-pGhFAD3-4-F4	This paper	N/A
PET28a-GhD53	This paper	N/A
GST-GhSLRF	This paper	N/A
PET28a-GhD53-P-loop	This paper	N/A
GST-GhSLRF-CAT	This paper	N/A

(Continued on next page)

Continued

REAGENT or RESOURCE	SOURCE	IDENTIFIER
104-GhD53	This paper	N/A
106-GhSLRF	This paper	N/A
104-GhD53-P-loop	This paper	N/A
106-GhSLRF-CAT	This paper	N/A
pYES2-FAD3-2	This paper	N/A
pYES2-FAD3-4	This paper	N/A
BD-GhD53	This paper	N/A
AD-GhSLRF	This paper	N/A
AD-GhSLRF-bHLH	This paper	N/A
BD-GhD53-P-loop	This paper	N/A
1300-GhSLRF	This paper	N/A
1300-GhD53	This paper	N/A
1300-GhFAD3-2	This paper	N/A
1300-GhFAD3-4	This paper	N/A
Software and algorithms		
MEGA7.0	This paper	N/A
ggplot2 3.2.0	RStudio	https://cran.r-project.org/web/packages/ggplot2/index.html
ClueGO 2.5.8.	Molecular Evolutionary Genetic Analysis	https://www.megasoftware.net/
TBtools v1.098661.	TBtools	https://github.com/CJ-Chen/TBtools/releases
DNAMAN 6.0.3.40	Cytoscape	https://apps.cytoscape.org/apps/cluego
Roche Light Cycle 480 II	Roche	https://lifescience.roche.com/en_fr/products/lightcycler14301-480-softwareversion-15.html
Illumina HiSeq2000	This paper	https://support.illumina.com/sequencing/sequencing_instruments/hiseq_2000/documentation.html
IGV 2.12.0	This paper	https://software.broadinstitute.org/software/igv/2.12.x
Other		
confocal microscope	Leica	TCS SP8 STED
CO ₂ critical point drying	CPD	Bal-Tec CPD 030
gold-palladium alloy	Zeiss	Zeiss-M2
scanning electron microscope	Hitachi	TM3030Plus
RNA-seq data of fibers treated with GR24 or Tis108	This paper	https://www.ncbi.nlm.nih.gov/bioproject/PRJNA871199/
The RNA-seq data of <i>GhD53</i> and <i>GhSLRF</i> transgenic cotton fiber	This paper	https://www.ncbi.nlm.nih.gov/bioproject/?term=PRJNA1015026
ChIP-seq data of 5 DPA fibers from <i>GhD53</i> and <i>GhSLRF</i> transgenic cottons	This paper	https://www.ncbi.nlm.nih.gov/bioproject/?term=PRJNA1014915
DAP-seq data of GhD53 protein	This paper	https://www.ncbi.nlm.nih.gov/bioproject/?term=PRJNA1029020

EXPERIMENTAL MODEL AND STUDY PARTICIPANT DETAILS

Plant material and growth conditions

The wild-type upland cotton (J668 and Z49) and corresponding transgenic cotton lines were grown in a greenhouse under long-day conditions (14-h light/10-h dark cycle) at 28 °C. Three 15-day post-anthesis cotton balls from each line were collected and cotton balls from at least 10 plants per line were subjected to observation and weight detection. The tobacco were grown in a climate-controlled chamber under a long day condition (16 h light/8 h dark cycle) at 25 °C and 60 % humidity.

METHOD DETAILS

Cotton transformation

The overexpression and RNAi or knockout plasmids of *GhD53*, *GhFAD3-2*, *GhFAD3-4*, and *GhSLRF* were constructed with the corresponding primers listed in [Table S6](#). For *GhD53* and *GhFAD3-4* genetic transformation, the constructed plasmids were introduced into the LB4404 *Agrobacterium tumefaciens* strain to be used on J668 cotton seedlings. 5-7 mm hypocotyls from the seedlings were incubated with the *A. tumefaciens* suspension (OD600 = 0.1-0.5) for 20 min, and then transferred onto a callus induction medium after blotted dry on sterilized filter papers. After callus induction, proliferation, embryogenic callus induction, embryo differentiation, and plantlet regeneration, the putative transgenic plants were transferred to pots and grown in a greenhouse at 28 °C under a long-day (14-h light/10-h dark) cycle.

For *GhFAD3-2* and *GhSLRF* genetic transformation, the constructed plasmids were introduced into EHA105 *A. tumefaciens* strain to be used on Z49 cotton embryos. Briefly, cotton embryo tips were incubated with *A. tumefaciens* suspension (OD600 = 0.1-0.5) for 30 min and transferred onto a culture medium for co-culture for 3 d at 23 °C. After co-culture, the embryos were transferred to another culture medium at 28 °C for 7 d, then placed on a screening medium containing spectacular mycin. After being cultured for 6 weeks, the resistant buds were induced, and the samples were transferred to an elongation medium for 3-6 weeks at 28 °C until rooting.⁴⁴

Cotton ovule culture

The cotton ovules were collected from *in vitro* ovule culture after one day of fertilization. The ovules were first sterilized in 10% sodium hypochlorite solution, peeled out in a sterile environment and cultured separately on a fluid nutrient medium (272.18 mg/L KH₂PO₄, 6.183 mg/L H₃BO₃, 0.242 mg/L Na₂MoO₄·2H₂O, 441.06 mg/L CaCl₂·2H₂O, 0.83 mg/L KI, 0.024 mg/L CoCl₂·6H₂O, 493 mg/L MgSO₄·7H₂O, 16.902 mg/L MnSO₄·H₂O, 8.627 mg/L ZnSO₄·7H₂O, 0.025 mg/L CuSO₄·5H₂O, 5055.5 mg/L KNO₃, 8.341 mg/L FeSO₄·7H₂O, 11.167 mg/L Na₂EDTA, 0.492 mg/L nicotinic acid, 0.822 mg/L pyridoxine·HCl, 1.349 mg/L thiamine·HCl, 180.16 mg/L myo-inositol, 18016 mg/L D-glucose and 3603.2 mg/L D-fructose. The pH = 6.0).^{26,27,45} The medium was added with 15 μM GR24, 10 μM Tis108, 5 μM C18:3 or 0.5 μM carbenoxolone (C18:3 biosynthesis inhibitor), and ovules in the medium were cultured for 10 d.

RNA extraction and RT-qPCR analysis

Total RNA from fibers and ovules were extracted using an RNA isolation kit (Tiangen) by following the manufacturer's instructions. First-strand complementary DNA (cDNA) strands were reverse-transcribed from the total RNA using a kit (Takara). The RT-qPCR was performed using gene-specific primers listed in the [Table S6](#). *GhUBQ7* (GenBank No. AY189972) was used as the internal control. The reactions were performed using the Roche LightCycler® 480 II instrument (Roche). The 2^{-ΔΔCT} method was used to calculate the relative expression levels of the target genes. Three independent biological replications were carried out for each gene in the RT-qPCR analysis.

Protein extraction and western blot

Total proteins were extracted from 10-DPA fibers using a protein extraction buffer (20 mM Tris-HCl (pH 7.5), 150 mM NaCl, 1 mM EDTA, 2% Triton-100, and protein inhibitor (Roche)). The protein was quantified by the Bradford method.⁴⁶ Equal amounts of protein from transgenic and wild-type plants were subjected to SDS-PAGE followed by western blot analysis. The anti-Flag (1:1,000, Sangon) and HRP-conjugated anti-mouse secondary antibody (1:10,000, Sangon) were used for immunodetection. The actin loading control was detected by using anti-actin mouse antibody (1:1,000, Sangon) and HRP-conjugated anti-mouse secondary antibody (1:10,000, Sangon).

ChIP-seq and ChIP-qPCR

Cotton fibers of 5-10 DPA from *GhD53-Flag-OE* and *GhSLRF-Flag-OE* cotton plants were used for ChIP assay. The 2 g of fiber and ovules were incubated in the cross-linking buffer (1% (v/v) formaldehyde) under a vacuum for 5 min at 4 °C and this step was repeated for six times. Then, the crosslinking was stopped by adding 2 M glycine under vacuum for 5 min. After that, fiber samples were ground into a powder in liquid nitrogen. The chromatin complexes were isolated, sonicated to 250-500 bp DNA strands, and incubated with the anti-Flag antibodies (1:1,000, Sangon). After overnight incubation at 4 °C, the immune complexes were eluted, and the DNA strands were purified for Illumina sequencing and qPCR. The library was sequenced using the Illumina HiSeq3000 platform at Beijing Novel Bioinformatics Co., Ltd. (<https://en.novogene.com/>). Sequencing data was mapped to cotton genome (*Gossypium hirsutum*, NAU). The ChIP-seq peaks in the promoter region were visualized using IGV 2.12.0 software (Integrative Genomics Viewer).^{47,48}

DAP-seq assay

The genomic DNA of cotton was extracted from 1 g of young leaves using a DNA isolation kit (Tiangen, Beijing, China). A DNA library was generated with a DNA Library Prep Kit (Vazyme) according to the manufacturer's instructions. The coding sequence of *GhD53* was amplified and cloned into pET-28a with His-tag and expressed in the BL21 *E. coli* strain. The purified *GhD53* protein was incubated with the genomic DNA library for 1 h. The eluted DNA strands were sequenced by the Wuhan IGenebook Biotechnology Co. Ltd (<http://www.igenebook.com/>). The primers used in this experiment are listed in [Table S6](#).

Subcellular location

The coding sequences of *GhD53*, *GhFAD3-2*, *GhFAD3-4*, and *GhSLRF* fused with GFP were amplified and cloned into *pCAMBIA1300*. The constructed plasmids were introduced into *GV3101 A. tumefaciens* and then *GV3101 A. tumefaciens* (OD600 = 1.2) with subcellular location plasmids were injected to the whole tobacco leaves, and injected tobaccos were growth at 25 °C under dark condition for 24 hours, then placed into a greenhouse at 25 °C under 16-h light/8-h dark cycle for 2 days.³ Confocal laser scanning microscopy (Olympus) was used to detect the fluorescence signals. *1300-GhBES1-mCherry* was used as a nuclear marker, and *pCAMBIA1300* with *AtCBL1* fused with mCherry was used as a membrane marker. All experiments were performed with three independent biological replicates, and the primers used in this experiment are listed in [Table S6](#).

Yeast one-hybrid assay

The conserved domains of *GhD53* and *GhSLRF* were predicted via the online InterProScan software (<https://www.ebi.ac.uk/interpro/about/interproscan/>). The coding sequence of *GhSLRF* was cloned into the *pGADT7* prey vector, and the 1,753 bp *GhFAD3-2* and 1,720 bp *GhFAD3-4* promoter sequences were inserted into the *pAbAi* bait vector and co-transformed to *Y1H Gold* yeast strain. Transformed yeast cell suspensions were dropped onto an SD [DDO for -Leu, with or without 500 ng/ml Aureobasidin A (AbA)] medium and cultured in the dark at 30 °C for 3 d. The protein-DNA interactions were then determined based on the growth of the co-transformants on the SD/-Leu medium containing AbA.

The *GhD53* and *GhSLRF* coding sequences and sequences encoding different conserved domains were cloned into the *pJG45* vector, the 1,753 bp *GhFAD3-2* and 1,720 bp *GhFAD3-4* promoter sequences, and the corresponding DNA fragments (with or without the binding site mutant) were inserted into the *pLacZi* vector. The respective combinations of activation domain-fusion effectors and *pLacZi* reporters were co-transformed into *EGY48* yeast strain, and transformants were selected and grown on SD/-Trp-Ura dropout media containing X-gal (5-bromo-4-chloro-3-indolyl-b-D-galactopyranoside). Yeast transformation and liquid assay were conducted as described in the Yeast Protocols Handbook (Clontech). All primers used for the yeast one-hybrid assays are listed in [Table S6](#).

Dual-luciferase (Dual-LUC) reporter assay

The dual-luciferase reporter assay was performed using *N. benthamiana* leaves and cotton protoplast. The *GV3101 A. tumefaciens* (OD600 = 1.2) with Dual-luciferase (Dual-LUC) reporter plasmids were injected to the whole tobacco leaves, and injected tobaccos were growth at 25 °C under dark condition for 24 hours, then placed into a greenhouse at 25 °C under 16-h light/8-h dark cycle for 2 days.³ The 1,753 bp *GhFAD3-2*, 1,720 bp *GhFAD3-4*, and corresponding fragments of promoter regions were cloned into the *pGreenII 0800-LUC* vector to generate the reporter construct.

In *N. benthamiana* leaves assay, the full-length coding sequence of *GhD53*, *GhSLRF*, and sequences encoding different conserved domains were cloned into the *pGreenII 62-SK* vector to generate the effector construct. Effector and reporter plasmids were then co-transformed into tobacco leaves for the luciferase activity assay. The intensity of the firefly luciferase bioluminescence was observed using an imaging system (Xenogen IVIS 100, PerkinElmer), and the luciferase activity was measured using the Dual-Luciferase® Reporter Assay System (Promega). The primers used in this experiment are listed in [Table S6](#).

Electrophoretic mobility shift assay (EMSA)

The promoter fragments from *GhFAD3-2* or *GhFAD3-4* with intact or mutated *GhD53* binding site or *GhSLRF* binding site were synthesized and labeled with biotin probes. The *GhD53* and *GhSLRF* coding sequences were cloned into *pET-28a* and expressed in the *BL21 E. coli* strain. The recombinant *GhD53* and *GhSLRF* proteins were purified using a His-tagged Fusion Protein Purification kit (Thermo Fisher Scientific) according to the manufacturer's instructions. EMSA assays were performed using a Chemiluminescent EMSA kit (Beyotime) following the manufacturer's instructions, and fluorescence was observed with an image scanner (Tanon). The primers used in this experiment are listed in [Table S6](#).

Yeast two-hybrid assay

The coding sequence of *GhSLRF* and the sequences encoding different conserved domains were amplified and inserted into the *pGADT7* vector, and the coding sequence of *GhD53* and corresponding conserved domain-related sequences were cloned into the *pGBKT7* vector. Empty vectors for *pGADT7* and *pGBKT7* were used as the negative control, and *pGADT7-T* and *pGBKT7-53* were used as positive control. The recombinant plasmids of *pGADT7* and *pGBKT7* were co-transformed into the *AH109* yeast strain. Yeast was grown on a selection plate (SD/-Trp/-Leu) (Coolab) for 3 – 4 d, and the interaction was detected on SD/-Ade/-His/-Leu/-Trp (Coolab) selective plates at 30 °C. The primers used in this experiment are listed in [Table S6](#).

BiFC assay

The coding sequence of *GhSLRF* and the sequences encoding different conserved domains were amplified and inserted into the *pXY106-nYFP* vector, and the coding sequence of *GhD53* and corresponding conserved domain-related sequences were cloned into the *pXY104-cYFP* vector. The recombinant plasmids of *pXY106-nYFP-GhSLRF* and *pXY104-cYFP-GhD53*, *pXY106-nYFP-GhSLRF-ACT* and *pXY104-cYFP-GhD53-P-loop* vectors were then co-transformed into tobacco leaves via

Agrobacterium-mediated transformation, respectively. After a 3-d culture, fluorescence signals were observed in an Olympus FV1200 (Olympus) confocal laser scanning microscope at 514 μ m. Fluorescence images were analyzed to determine the binding sites. The primers used in this experiment are listed in [Table S6](#).

Co-IP assay

The coding sequence of *GhD53* and corresponding conserved domain-related sequences were fused to a Flag-tag and cloned into pCAMBIA1305-Flag vector, and the coding sequence of *GhSLRF* and corresponding conserved domain-related sequences were cloned into a pCAMBIA1300-GFP vector. The constructed plasmids were then introduced into *A. tumefaciens* GV3101 and then transiently transfected in tobacco leaves. After 2 d, the leaf proteins were extracted using an extraction buffer (pH 7.5; 100 mM Tris-HCl, 5 mM EDTA, 100 mM NaCl, 1.0 % Triton-X-100, 0.5 mM PMSF, and protease inhibitor cocktail (Sigma)). Pierce Protein A/G Magnetic Beads (Thermo Fisher Scientific) and anti-GFP antibody were incubated with the proteins at 4 °C for 5 h. The Co-IP products were then washed gently five times using a wash buffer (pH 7.5; 150 mM NaCl, 1 mM EDTA, 1.0 % Triton-X-100, 0.5 mM PMSF, protease inhibitor cocktail, and 20 mM Tris-HCl). The *GhD53*-Flag and P-loop-Flag domain proteins were detected by immunoblotting with anti-Flag antibody (1:1,000, Sangon), and anti-GFP antibody (1:1,000, Sangon), and the chemiluminescence signal was detected using autoradiography via an image scanner (Tanon). The primers used in this experiment are listed in [Table S6](#).

Pull-down assay

The *GhD53* coding sequence and P-loop domain coding sequence were cloned into the pET-28a vector with a -tag, and the coding sequences of the *GhSLRF* and ACT domain coding sequence were cloned into the pGEX-6P-1 vector with a GST tag, respectively. The *GhD53*-His and P-loop-His fusion proteins were expressed in BL21 *E. coli* grown at 16 °C in the presence of 0.1 mM IPTG (isopropyl β-D-1-thiogalactopyranoside), while the *GhSLRF*-GST and ACT-GST fusion proteins were grown at 20 °C in the presence of 0.3 mM IPTG. The primers used in this experiment are listed in [Table S6](#).

For the *in vitro* pull-down assays, the 10 μ g GST tag-fused *GhSLRF* protein and ACT domain protein were incubated with GST-binding resin (GenScript, L0026, Nanjing, China) at 4 °C for 2 h. After the resin was washed with phosphate-buffered saline, the 2 μ g of purified His tag-fused *GhD53* and P-loop domain protein were added and incubated at 4 °C for another 4 h. Then the resin was washed for more than three times with Lysis buffer (25 mmol/L Tris, 150 mmol/L NaCl, 0.1 % NP40, 0.1 g/mL lysozyme, 1 mmol/L PMSF, pH 7.5). The eluted proteins were then analyzed by immunoblotting using anti-His (1:1,000, Sangon) and anti-GST (1:1,000, Sangon) antibodies. The chemiluminescence signal was detected using autoradiography via an image scanner (Tanon 4800, Tanon, China).

RNA-seq analyses

Total RNA was extracted from 10-day-old fibers treated with GR24, the corresponding inhibitor Tis108, or 10-day-old control fibers (CK) using the Invitrogen RNeasy kit. (Life Technologies, USA). For RNA library construction, and 2 mg RNA per sample was used to construct RNA-seq libraries using NEBNext UltraTM RNA Library Prep Kit for Illumina (New England Biolabs, Ipswich, MA, USA) described in the kit's manual. Illumina Hiseq platform (HiSeq 2000) was used to generate 125/150 bp paired-end sequence reads.²⁶ The differential expression analysis was performed by DESeq2⁴⁹ software between two different groups. The genes with the parameter of false discovery rate (FDR) below 0.05 and absolute fold change \geq 2 were considered differentially expressed genes (DEGs). The bioinformatic analysis was performed using the Omicshare tools (<https://www.omicshare.com/>). RNA-seq data was available in NCBI with accession number PRJNA1015026.

Fatty acid content detection

The fatty acid contents of fiber cells were measured at Qingdao Ke Chuang company (<https://www.zhaowoce.com/institution/15483458.html>). Briefly, 10-d fiber is soaked in chloroform/methanol (2:1, v / v) for 1 min to remove the surface wax. Then they were ground into a powder in liquid nitrogen and extracted 3 times with ethanol: water: diethyl ether: pyridine: ammonium hydroxide (7.0 N) (15:15:5:1:0:18, v/v). Heptadecanoic acid (C17:0, Sigma-Aldrich) was added to the fatty acid extraction medium to monitor the recovery and quantification of fatty acids, dried under nitrogen, and heated in H₂SO₄ (3 N) to 85 °C for 5 h derivatization. After returning to room temperature, fatty acid methyl ester was extracted with hexane 3 times and concentrated to the final volume of 200 μ L. Fatty acid concentrations were measured using a GC tandem mass spectrometry system, briefly, the fatty acid methyl esters were dissolved in hexane, and 1 μ L sample was injected into the Agilent 6890N GC system (Agilent, California, USA). Fatty acids were measured by an HP 5975 mass selective detector (HP, California, USA) connected to the GC system.⁵⁰

Microscopic analysis

Thirty 0-DPA cotton ovules were collected to investigate their fiber cell initiation. A scanning electron microscope (Hitachi) was used to image the fiber initiation according to the standard method described in the instruction manual.

Phylogenetic, sequence alignment and domain analysis

The phylogenetic tree was constructed using MEGA 7.0.26 with neighbor-joining method and 1,000 bootstrap replicates. The protein sequences of GhFAD3-2 and GhFAD3-4 were aligned using the ClustalW method⁵¹ and visualized by the BioEdit 7.1.3.0 software.⁵² The conserved domains of GhD53 and GhSLRF were predicted using the InterProScan online website (<https://www.ebi.ac.uk/interpro/search/sequence/>).

QUANTIFICATION AND STATISTICAL ANALYSIS

Quantification and statistical analyses were performed using GraphPad. All data are presented as Mean and Standard Deviations (SD). *p* value was calculated through two-tailed paired Student's *t*-test. *p* < 0.05 was considered statistically significant. 0.01 < *p* < 0.05 is defined as one asterisk (*), 0.001 < *p* < 0.01 is defined as two asterisks (**) and *p* < 0.001 is defined as three asterisks (**). Details of statistical analysis are indicated in corresponding figure legends (with error bars, exact value of *n*, and the statistical analysis).